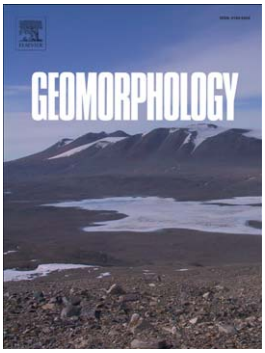


# Fractal features of soil particle size distribution in layered sediments behind two check dams: Implications for the Loess Plateau, China

Xia Wei, Xungui Li

PII: S0169-555X(16)30265-3
DOI: doi: 10.1016/j.geomorph.2016.05.003
Reference: GEOMOR 5594

To appear in: *Geomorphology*

Received date: 17 November 2014
Revised date: 4 January 2016
Accepted date: 2 May 2016

Please cite this article as: Wei, Xia, Li, Xungui, Fractal features of soil particle size distribution in layered sediments behind two check dams: Implications for the Loess Plateau, China, *Geomorphology* (2016), doi: 10.1016/j.geomorph.2016.05.003

# Fractal features of soil particle size distribution in layered sediments behind two check dams: implications for the Loess Plateau, China

Xia Wei  Xungui Li*

Key Laboratory of Western China's Environmental Systems (Ministry of Education), College of Earth and Environmental Sciences, Lanzhou University, 222 South Tianshui Road, Lanzhou, Gansu Province 730000, China

*Corresponding author. Tel: 86-13679484701

E-mail: lixung@lzu.edu.cn (X. Li)

**Abstract**: The layered sediment deposited behind a check dam can provide useful information about soil erosion processes in the dam-controlled area. This study aims to evaluate the possible fractal nature of layered sediments behind check dams, assessing whether fractal dimension can serve as a feasible index for evaluating the impact of land use types on the area controlled by the check dam. Fractal dimension measurement was employed to analyze the features of soil particle size distribution (PSD) for different layered sediments of the Shipanmao and Zhangshan check dams in the Dalihe River Basin of the Loess Plateau, China. Results show that the predominant soil particle sizes of the sediment layers behind the Shipanmao and Zhangshan dams are silt–clay (<0.05 mm) and fine sand (0.25–0.05 mm). The overall gradients of the trends for silt–clay and fine sand are 0.0622 (slight increase) and −0.0618 (slight decrease), respectively, for Shipanmao, and −0.8415 (decrease) and 0.8448 (increase), respectively, for Zhangshan. There are considerable differences in the PSDs among different layers, especially in the coarse and fine sand fractions. The coefficient of variation (*CV*) for the coarse sand fraction is highest, followed by the fine sand and the silt–clay size fractions. Larger soil particle sizes coincide with larger *CV* values. The fractal dimension ($D_m$) of the PSD ranges from 2.111 to 2.219, and 2.144 to 2.447 for Shipanmao and Zhangshan, respectively. The $D_m$ values tend to increase and decrease for the layered sediments from top to bottom with some turning points. The turning points of $D_m$ are related to the trends of the soil PSDs in the adjacent sediment layers. Although $D_m$ has significant positive and negative correlations with the silt–clay and the fine sand size fractions, respectively, no

correlation with the coarse sand fraction was observed. Soil PSD is a more dominant factor affecting $D_m$ than the time lag between soil erosion and sediment deposition. Overall, $D_m$ decreased for Shipanmao during the deposition period (1972–1979). The total increment of the *C* factor in the universal soil loss equation and the soil erosion amount per rainfall erosivity were applied to analyze land use changes between 1972 and 1979 for the dam-controlled area of the Shipanmao dam. The total increment of *C* during 1972–1979 was 0.021 and the soil erosion amount per rainfall erosivity was smaller in 1972 than in 1979, indicating desertification in the dam-controlled area. In addition, the land use types prevalent in 1979 were more prone to soil loss than those in 1972. $D_m$ is a useful parameter to assess land use types and soil degradation processes in dam-controlled areas of the Loess Plateau.

**Keywords**: Soil particle size distribution; fractal dimension; land use types; check dam

## 1. Introduction

Soil erosion is one of the most serious environmental issues in China (Shi and Shao, 2000; Zheng, 2006; Li et al., 2011; Li and Wei, 2014). It affects an area of 3.6 million $km^2$, equal to about 37% of the country's total land area (MWR, 2002). Water, wind, and freeze-thaw erosion of soils are widely distributed in China, causing soil deterioration (Marques et al., 2008; Fu et al., 2011; Jebari et al., 2012), decline in land productivity (Pimentel and Kounang, 1998; Lantican et al., 2003; Fu et al., 2011), and degradation of streams, lakes, and estuaries through transportation and settling of sediments and pollutants (Li and Wei, 2014). The Chinese Loess Plateau in particular has suffered from serious soil erosion in recent decades (Zhang et al., 1998; Shi and Shao, 2000; Li and Wei, 2014) due to intensive human disturbance and the presence of thick erodible soil (Shi and Shao, 2000; He et al., 2004). Erosion from the Loess Plateau, which is the main source area of sediment discharging into the Yellow River (Ren and Shi, 1986; Shi and Shao, 2000; Xu, 2003), contributes about 30% of the total soil loss in China (MWR, 2002). Soil loss is also a major environmental problem threatening the sustainable development of the Loess Plateau (Ni et al., 2008; Feng et al., 2010; Liu et al., 2012).

To mitigate the severe soil erosion in this region, a number of soil and water conservation measures have been adopted such as revegetation, tillage management, enclosures, terracing, and check dams (Creamer et al., 1997; Valentin et al., 2005; Lu et al., 2012). Among these measures, check dams, manmade structures built across a channel to reduce stream speed and trap sediment (Hudson, 1981; Creamer et al.,

1997; Chanson, 2004; Zeng et al., 2009), are often the most efficient engineering approaches toward sediment retention (Creamer et al., 1997; Xu and Sun, 2004; Ran et al., 2008; Li and Wei, 2011; Lu et al., 2012; du Plessis et al., 2015; Sylvain et al., 2015). They are popular on the Chinese Loess Plateau and have a long history of construction and use (Fang et al., 1998; Hu et al., 2002; Jiao et al., 2003; Li, 2003; Zeng et al., 2009). The speed and magnitude of check dam development on the Loess Plateau has been accelerated in the last 50 years with the support of the Chinese government (Li and Wei, 2011; du Plessis et al., 2015), leading to a reduction in sediment yield, soil and water conservation (Foncin, 1996; MartiFabregas, 1996; Magiera, 1997; Jiao et al., 2001; Jiao et al., 2003; Ran et al., 2004; Xu and Sun, 2006), and increased stability of dam systems (Coppens and Kato, 1997).

Sediments behind a dam are soils eroded in the dam-controlled area, including top and deeper soils depending on land use types such as sloping farmland and abandoned grazing land subject to rainfall and runoff. On the Loess Plateau, the area of sediment deposition behind a check dam (hereafter referred to as dam land, following the terminology of local farmers) is often formed by several rainfall events causing erosion in the dam-controlled area. The area of sediment deposition in a dam land is often flat and more fertile compared with the sloping land. Local farmers prefer to plant corps there and obtain 8- to 10-times more yield than on the sloping land (Fang, 1996; Xu et al., 2006).

The peak of sediment deposition and the flood peak tend to be synchronized in this region at the watershed scale (Chen et al., 1988; UMYRBYRCC, 2000; Tang,

2004; Wei et al., 2006b; Li and Wei, 2014), with larger floods producing more sediment, although a time lag between eroded soil sources and final sediment destination may exist, triggered by rainstorms with high intensity and short duration (Shi et al., 2012). Overall, however, sediment deposition behind the check dam reflects erosion in the upstream area (Zhang et al., 2007; Zhao et al., 2010a; Zhao et al., 2010b; Romero-Diaz et al., 2012; Hsieh et al., 2013). The problem of water and soil loss in the upstream area of a check dam, resulting from human influences such as land use, can be analyzed quantitatively using system theory (Li and Wei, 2011). However, there are few studies on the evaluation of land use types in areas controlled by check dams on the Loess Plateau.

Soil particle size distribution (PSD) is commonly used in the estimation of various related soil properties and for soil classification (Hillel, 1980). The PSD is one of the most important physical soil attributes (Prosperini and Perugini, 2008) due to its strong influence on movement and retention of water, solutes, heat, and air (Su et al., 2004). During soil erosion, a decrease in water-holding capacity, loss of soil nutrients, and depletion of soil structure are accompanied by selective removal of the fine particle size fractions (Lobe et al., 2001; Zalibekov, 2002; Su and Zhao, 2003; Su et al., 2004; Xu et al., 2013) by rainfall and runoff (Wang et al., 2008; Xu et al., 2013). Thus, identifying changes in PSD may provide useful insight into soil degradation caused by land use (Wang et al., 2008; Liu et al., 2009). Fractal theory has been applied to various geological phenomena that display large, scale-invariant, and self-similar characteristics since the 1980s (Mandelbrot, 1982; Katz and Thompson,

1985; Turcotte, 1986; Su et al., 2004; Wang et al., 2008; Liu et al., 2009; Xu et al., 2013). In addition, the possibility of characterizing PSD using fractal theory has been explored by several researchers (Tyler and Wheatcraft, 1992; Su et al., 2004; Xu et al., 2013; Yu et al., 2015). Fractal dimension becomes a useful measurement to quantitatively describe soil structure, soil erodibility, water permeability, and related soil properties (Perfect and Kay, 1995; Perfect, 1997; Su et al., 2004; Xia et al., 2015; Yu et al., 2015). Soil science has successfully utilized fractal methods to shed new light on soil degradation/desertification and complex dynamics of soil forming processes by studying PSD (Pachepsky et al., 1995; Su et al., 2004; Prosperini and Perugini, 2007; Xu et al., 2013). Fractal information may reveal sediment deposition processes and facilitate the choice of soil and water conservation measures and land use types in dam-controlled areas of the Loess Plateau (Wang et al., 2008; Liu et al., 2009). However, so far, there are only few reports on the application of fractal theory to analyze soil PSD of layered sediments in the dam land behind check dams and to determine the effects of human activities on soil erosion from the dam-controlled area. In fact, whether the PSD of layered sediment in dam lands has fractal characteristics is still unknown.

This study aims to evaluate the fractal nature of layered sediments in the dam lands of the Shipanmao and Zhangshan check dams, located in the Xiaohegou and Hongheze watersheds of China's Loess Plateau. Fractal dimension ($D_m$) was measured and the relationship between PSD of layered sediment and $D_m$ was evaluated to assess the desertification trend of the dam-controlled area. Then the

applicability of $D_m$ to analyze the impact of land use types in the dam-controlled area was evaluated.

## 2. Materials and methods

### *2.1. Study area*

The Xiaohegou and Hongheze watersheds are located at N37°36′17″ to N37°43′34″ and E109°47′42″ to E109°56′10″, and N36°42′23″ to N36°45′20″ and E108°53′30″ to E109°02′00″, respectively (Fig. 1). They are situated along tributaries of the Dalihe River, whose water flows into the Yellow River. The Xiaohegou and Hongheze watersheds cover an area of 63.5 and 76.2 $km^2$ with average gradients of 1.42% and 3.60%, respectively (SWCB, 2003; Li et al., 2007). The topography of both watersheds is characterized by low mountains and hills. The elevation ranges from 921 m above sea level (a.s.l.) in the southwest to 1,249 m a.s.l. in the northeast for the Xiaohegou watershed and from 1,233 m a.s.l. in the southeast to 1,606 m a.s.l. in the northwest for the Hongheze watershed. They are characterized by an arid to semiarid monsoon climate. According to the nearest Caoping hydrological station, the average annual temperature and precipitation are 9.79°C and 421 mm, respectively (Fig. 2), with 69.8% of rainfall occurring between June and September. Typical loess soils are commonly found, and the annual average erosion modulus and sediment discharge from the watershed are 15,000 t $km^{-2}$ $yr^{-1}$ and 922,500 t, respectively, for the Xiaohegou watershed (SWCB, 2003), and 13,500 t $km^{-2}$ $yr^{-1}$ and 739,000 t,

respectively, for the Hongheze watershed (Wei et al., 2006a). The two watersheds are located in sub-region I of soil erosion regions of the Loess Plateau as defined by Meng (1996), corresponding to the area of severest soil erosion.

*2.2. Soil sampling*

The Shipanmao and Zhangshan check dams were built in 1972 and 1974, and damaged by rainstorms in 1979 and 1989, respectively. The sampling locations were positioned in the dam land about 5 m upstream from the two dams. Soil sampling sites were dug with a shovel. The total thicknesses of the deposited sediments are 6.28 m for the Shipanmao check dam covering the period of 1972–1979 and 7.89 m for the Zhangshan check dam for 1974–1989. The number and thickness of sediment layers formed by rainstorms and floods are mainly influenced by storm intensity, rainfall amount, basin topography, land cover, soil texture, and degree of land use. A layer from a single rainstorm and flood can be identified based on the layer structure of the sediment (Fig. 3). We divided the 6.28-m thick soil profile from the Shipanmao dam land into 21 layers and the 7.89-m thick soil profile from the Zhangshan dam land into 17 layers. We only linked the sediment layers from Shipanmao to rainstorm events recorded during 1972–1979 at Caoping station (Table 1). For the Zhangshan dam, we did not link the sediment layers to the rainstorm events because Caoping station is too far from Zhangshan (Fig. 1) and no adjacent stations are available.

Soil samples were collected from each depositional layer using a soil sampling auger with a diameter of 5.0 cm. Three soil samples were taken from each layer and

combined to obtain a composite sample. The samples were air-dried and machine-sieved through a 2-mm screen to remove roots and other debris. The PSD was measured by laser diffraction using a Mastersizer2000 particle size analyzer (Malvern Instruments, Malvern, England) and described for each sample in terms of the percentage of silt and clay (<0.05 mm), fine sand (0.05–0.25 mm), coarse sand (0.25–1.0 mm), and gravel (1.0–2.0 mm).

*2.3. Measurement of soil fractal dimension*

For fractal scaling of PSD, the cumulative number of soil grains $r$ greater than a characteristic size (specific measuring scale) $R$ is set to be $N(r > R)$ and the cumulative mass distribution of soil grains $r$ smaller than the specific measuring scale $R$ is set to be $M(r < R)$. Then, the values of $N(r > R)$ and $M(r < R)$ will be proportional to $R^{D\mathrm{m}}$ and $R^{3-D\mathrm{m}}$, respectively (Tyler and Wheatcraft, 1992).

The exponent $D_\mathrm{m}$ can be easily determined based on the relationship between $R$ and $N(r > R)$ or $M(r < R)$ (Turcotte, 1986; Tyler and Wheatcraft, 1992). Mandelbrot (1982) suggested that fractal fragmentation could be quantified based on the relationship between the number and size in a statistically self-similar system:

$$N(X \geq x_i) = k x_i^{-D_\mathrm{m}} \tag{1}$$

where $N(X \geq x_i)$ is the cumulative number of objects or fragments $X$ greater than the $i$-th characteristic size $x_i$ and $k$ is the number of elements at a unit length scale.

However, the relationship given by Eq. (1) is not convenient and errors can be introduced in the calculations (Prosperini and Perugini, 2008). The applicability of Eq. (1) to the PSD analysis is also limited because $N$ values are unavailable in conventional PSD data. To compensate for the lack of $N$ values, Turcotte (1986) and Tyler and Wheatcraft (1992) presented an estimation of $D_m$ for soil PSD:

$$M(r<R_i)/M_T = (R_i/R_{max})^{3-Dm} \quad (2)$$

where $R_i$ is the mean particle diameter (mm) of the $i$-th size class; $M$ is the cumulative mass of particles of size $r$ smaller than $R_i$; $M_T$ is the total mass and $R_{max}$ is the mean diameter of the largest particle. The mean diameter is the arithmetic mean of the upper and lower sieve sizes (Liu et al., 2009).

Taking the logarithm of both sides of Eq. (2) yields the following equation:

$$\log[M(r<R_i)/M_T] = (3-D_m)\log(R_i/R_{max}) \quad (3)$$

From the linear regression between $\log[M(r < R_i)/M_T]$ and $\log(R_i/R_{max})$ in Eq. (3), the value of $3 - D_m$ can be determined. If the slope of the regression is denoted as $k_s$, the value of $D_m$ can be determined by:

$$D_m = 3 - k_s \quad (4)$$

*2.4. Assessment criterion for land use type changes*

Because soil erosion is associated with land use/crop cover (Boardman et al., 2009) and the *C* factor in the universal soil loss equation (USLE) has important influence on the soil erosion risk (Ozcan et al., 2008; Zhou et al., 2008; Li and Wei, 2014), the *C* factor can be determined based on land use (Kefi et al., 2012). For more details about the USLE, please see Wischmeier and Smith (1958, 1965, 1978), Risse et al. (1993), Rapp et al. (2001), Suri et al. (2002), Shrestha et al. (2004), Kinnell (2005), Wu and Wang (2007), and Li and Wei (2014).

The following equation is used to determine the total increment of the *C* factor in the dam-controlled area during a given period:

$$\Delta C_{\mathrm{T}} = \sum_{i=1}^{n} C_i \frac{A_i}{A_{\mathrm{T}}} \tag{5}$$

where $\Delta C_{\mathrm{T}}$ is the total increment of the *C* factor in the dam-controlled area during the period; $n$ is the total number of land use types; $C_i$ is the *C* factor of the $i$-th land use type; $A_i$ is the area increment of the $i$-th land use type; and $A_{\mathrm{T}}$ is the area controlled by the check dam.

According to the definition of the *C* factor (Laflen and Moldenhauer, 2003), a land use type with a larger *C* factor is more prone to soil erosion. Thus, if the value of $\Delta C_{\mathrm{T}}$ is larger than zero, it indicates that the land use types during a period become worse with regard to soil erosion; otherwise, the land use types become better.

Because rainfall erosivity is the most important factor influencing soil erosion on the Chinese Loess Plateau (Xu, 1998; Zheng et al., 2008; Li and Wei, 2014), an index for the amount of soil erosion per rainfall erosivity was employed to analyze the degree to which land use types influence soil erosion:

$$\beta = \frac{W_1}{R} \tag{6}$$

where $W_1$ is the total weight of a layer of deposited sediment in t; $R$ is the rainfall erosivity corresponding to $W_1$ in MJ mm hr$^{-1}$ ha$^{-1}$; and $\beta$ is the soil erosion volume per rainfall erosivity in t MJ$^{-1}$ mm$^{-1}$ hr ha. The bigger the value for $\beta$, the more severe the soil erosion due to a particular land use type.

The rainfall erosivity $R$ quantifies the ability of rainfall to cause soil loss from hillslopes (Yin et al., 2007), which is determined by (Wischmeier and Smith, 1978):

$$R = E \cdot I_{30} \qquad E = \sum_{r=1}^{n} (e_r \cdot P_r) \qquad e_r = 0.29\left[1 - 0.72\exp(-0.05 i_r)\right] \tag{7}$$

where $R$ is rainfall erosivity in MJ mm hr$^{-1}$ ha$^{-1}$; $I_{30}$ is maximum rainfall intensity in 30 min in mm hr$^{-1}$; $E$ is rainfall kinetic energy in MJ ha$^{-1}$; $e_r$ is rainfall kinetic energy per minute in MJ ha$^{-1}$ mm$^{-1}$; $P_r$ is amount of rainfall corresponding to $e_r$ in mm and $i_r$ is the average rainfall intensity in mm hr$^{-1}$.

## 3. Results

*3.1. Soil PSDs and $D_m$*

The soil PSDs and $D_m$ of layered sediment for the Shipanmao and Zhangshan dam lands are shown in Tables 2 and 3, respectively. For the Shipanmao dam land, the predominant soil particle size is silt–clay, with a percentage ranging between 49.14% (Layer 8) and 82.81% (Layer 15) and a mean of 66.29%. The contents of fine sand and coarse sand are relatively low. The percentage of fine sand ranges between 17.03% (= 6.34% + 10.69%; Layer 15) and 50.85% (Layer 8), with a mean of 33.63%, and that of the coarse sand ranges from 0.01% (Layers 8 and 10) to 0.18% (Layer 13), with a mean of 0.08%. For the Zhangshan dam land, the soil PSDs for fine sand and silt–clay total more than 99.87%, similar to the 99.82% of the Shipanmao dam land. However, the average percentages of silt–clay, fine sand, and coarse sand are 49.60%, 50.35%, and 0.05% respectively, which are different from the 66.29%, 33.63%, and 0.08% of the Shipanmao dam land. No gravel was detected for the two dam lands. Soils are classified as yellow-brown soils (Haplumbrepts), according to the Chinese soil texture classification system (Lin, 2002).

Trends in the distribution of silt–clay (<0.05 mm) and fine sand (0.25–0.05 mm) in layers from the Shipanmao and Zhangshan dam lands are illustrated in Fig. 4. For the Shipanmao, the overall gradients of the linear trend lines for silt–clay and fine sand are 0.0622 (slight increase) and −0.0618 (slight decrease), respectively. When the percentage of silt–clay increases, the percentage of fine sand decreases. In contrast, the Zhangshan dam land shows opposite overall gradients for silt–clay and fine sand of −0.8415 (decrease) and 0.8448 (increase), respectively.

As shown in Tables 2 and 3, there are considerable differences in the PSD among the different sediment layers, especially for coarse and fine sands (see the coefficient of variation, *CV*, illustrated in Fig. 5). For the Shipanmao dam land, the *CV* value for coarse sand is highest (0.74), followed by fine sand (0.29), and silt–clay (0.15). The similar situation is found for the Zhangshan dam land. The larger the soil particle size, the bigger the *CV* value. The *CV* values for coarse sand, fine sand, and silt–clay from the Zhangshan dam land are bigger than those for sediments from the Shipanmao dam land.

The $D_m$ values of soil PSDs for the two dam lands were determined using Eq. (4) (Tables 2 and 3). The determination coefficients $R^2$ in Tables 2 and 3 are based on the linear regression of Eq. (4). Values for $R^2$ range between 0.84 (Layers 15 and 17) and 0.93 (Layers 11 and 18) for the Shipanmao dam land, and between 0.86 (Layer 2) and 0.97 (Layer 15) for the Zhangshan dam land, which are both significant at the 0.05 confidence level. The $D_m$ of the PSD ranges from 2.111 (Layer 11) to 2.219 (Layer 21) for the Shipanmao dam land, and from 2.144 (Layer 17) to 2.447 (Layer 2) for the Zhangshan dam land, with *CV* values of only 0.01 and 0.04 for the Shipanmao and Zhangshan dam lands, respectively, which indicates that the layers show no obvious fluctuations in fractal features. However, a weak increasing or decreasing tendency of $D_m$ from the top layers to the bottom layers is visible ($R^2$ = 0.1056 for the Shipanmao, and $R^2$ = 0.1542 for the Zhangshan; Fig. 6). Fig. 6 also demonstrates the existence of several turning points for $D_m$ (Layers 3, 4, 5, 11, 15, and 19 for the Shipanmao, and Layers 2, 4, 8, 10, and 11 for the Zhangshan; Fig. 7). For the Shipanmao dam land,

$D_m$ increases from Layer 1 to Layer 3 ($R^2$ = 0.9356; Fig. 7a) and then decreases to a valley in Layer 4. After reaching another peak in Layer 5, $D_m$ decreases from Layers 5 to 11 ($R^2$ = 0.8575). Then, $D_m$ shows an increasing trend from Layers 11 to 15, but decreases between Layers 15 and 19. For Layers 19 to 21, $D_m$ again shows an increasing trend. On the other hand, for the Zhangshan dam land, $D_m$ reaches a peak value of 2.447 in Layer 2 (from 2.211 in Layer 1) and then decreases for Layers 2 to 4 ($R^2$ = 0.9977; Fig. 7b). Between Layers 4 and 8, $D_m$ shows an increasing trend, and then decreases from Layers 8 to 10. After reaching another peak in Layer 11, $D_m$ again shows a decreasing trend from Layers 11 to 17.

Linear regression analysis was performed to determine the relationships between $D_m$ and the size fractions of coarse sand, fine sand, and silt–clay (Fig. 8). The $D_m$ of the PSD has a significant positive correlation with the silt–clay size fraction ($R^2$ = 0.5260, $p < 0.05$ for the Shipanmao dam land; $R^2$ = 0.6587, $p < 0.05$ for the Zhangshan dam land), a significant negative correlation with the fraction of fine sand ($R^2$ = 0.5259, $p < 0.05$ for the Shipanmao dam land; $R^2$ = 0.6588, $p < 0.05$ for the Zhangshan dam land), and no correlation with the coarse sand fraction ($R^2$ = 0.0117, $p > 0.05$ for the Shipanmao dam land; $R^2$ = 0.0880, $p > 0.05$ for the Zhangshan dam land). Soils with higher silt–clay content and lower fine sand content have higher $D_m$ values. The increase in $D_m$ of PSD as soil becomes finer matches the results of Liu et al. (2009) and Xu et al. (2013).

### *3.2. Temporal changes in $D_m$*

Based on the occurrence of erosive rainfall events, the corresponding soil PSDs and $D_m$ for the Shipanmao dam land shown in Table 2 were averaged to obtain annual values (Table 4).

The annual values of $D_m$ range from 2.139 in 1979 to 2.219 in 1972. Although the difference in $D_m$ is small with a *CV* value of 0.012, there exists a linear decreasing trend ($R^2$ = 0.4099; Fig. 9), significant at the 0.1 confidence level. In addition, the silt–clay percentage also shows a decreasing trend (Fig. 10), indicating that an increase in fine sand or a decrease in silt–clay can lead to a decrease in $D_m$.

*3.3. Changes in land use types*

When the Shipanmao check dam was built in 1972, the land use types in the dam-controlled area were sloped farmland, forest, grassland, terrace, and badland, with an area of 453,900, 618,600, 288,500, 162,700, and 480,800 $m^2$, respectively (Table 5). However, by the time the dam was damaged in 1979, the land use types had changed to sloped farmland (792,500 $m^2$), forest (573,000 $m^2$), grassland (32,800 $m^2$), terrace (182,700 $m^2$), dam land (14,400 $m^2$) and badland (409,100 $m^2$) (Table 5). Sloped farmland had a significant increase of 338,600 $m^2$, while grassland had a prominent reduction of 255,700 $m^2$.

This study adopts the *C* factor values from Li and Wei (2014), with *C* factors for dry farmland, forest, high coverage grassland, medium coverage grassland, low coverage grassland, and badland of 0.31, 0.006, 0.067, 0.120, 0.274, and 0.411, respectively. In this study, the *C* factors for forest and badland were set as 0.006 and

0.411, respectively (Table 5). Sloped farmland and terrace are considered dry farmland, with their *C* factors set as 0.310. Due to a lack of detailed data about the three kinds of grasslands (high, medium, and low coverage grasslands) in the study area, the *C* factor for grassland was determined as the average of the three kinds of grasslands, which is 0.154. For the dam land, the *C* factor is set as zero because it was formed by the eroded soil from the area controlled by the check dam and did not produce any additional soil erosion. The total increment ($\Delta C_T$) of the *C* factor in 1979 was calculated as 0.021 using Eq. (5). The land use types in 1979 resulted in a positive increment of the *C* factor.

For Layer 21, which resulted from a single rainstorm with a duration of 1767 minutes (29.45 hours) in 1972, the soil erosion amount per rainfall erosivity ($\beta$) is equal to 12.77 t $MJ^{-1}$ $mm^{-1}$ hr ha (= 236.74 t/18.54 MJ mm $hr^{-1}$ $ha^{-1}$) using Eqs. (6) and (7). For Layers 1 and 2, which resulted from two rainstorm events in 1979 with durations of 472 and 395 minutes (7.87 and 6.58 hours) respectively, the values for $\beta$ are 13.35 t $MJ^{-1}$ $mm^{-1}$ hr ha (= 80.21 t/6.01 MJ mm $hr^{-1}$ $ha^{-1}$) and 13.27 t·$MJ^{-1}$ $mm^{-1}$ hr ha (= 185.71 t/14.00 MJ mm $hr^{-1}$ $ha^{-1}$), respectively. Accordingly, the $\beta$ value for 1972 is smaller than that for 1979.

## 4. Discussion

### *4.1. Impact assessment of land use types in the dam-controlled area*

Some studies have reported that different soils have fractal characteristics. Su et

al. (2004), Liu et al. (2009), and Xu et al. (2013) found that natural soils have fractal characteristics. Wang et al. (2008) demonstrated that turbulent soils affected by human activities (land use) also have fractal features. Our study further found that layered sediments in dam lands also show fractal features. In addition, the relationship between $D_m$ and land use types was analyzed by some researchers. Su et al. (2004) found that the smaller the $D_m$ was, the more susceptible the land was to soil erosion. Wang et al. (2008) used a multi-fractal tool to analyze the characteristics of soil PSD for different land use types on the Loess Plateau, China. They found that the entropy dimension ($D_1$) and the ratio of entropy dimension ($D_1$) to capacity dimension ($D_0$) were significantly positively correlated to finer particle content and soil organic matter. The parameters of $D_0$, $D_1$, and $D_1/D_0$ were significantly influenced by land use type and may be potential parameters reflecting physical soil properties and soil quality influenced by land use types. Liu et al. (2009) analyzed the $D_m$ of soil PSD in the forested region of Mountain Yimeng, China and showed that a smaller $D_m$ corresponded to lower silt and clay contents and higher sand content, which the authors related to a change toward less favorable land use types. Xu et al. (2013) carried out research on the $D_m$ of PSD in a typical watershed in the source area of the middle Dan River, China and indicated that larger $D_m$ values corresponded to higher silt–clay contents. However, their results did not show fractal features of layered sediment of dam lands and their relation to land use type in dam-controlled areas of the Loess Plateau.

According to the changes of land use types and the values of the *C* factor in the dam-controlled area of the Shipanmao check dam (Table 5), the land use types prevalent in 1979 resulted in a positive increment of the *C* factor. This is demonstrated by the soil erosion amount per rainfall erosivity ($\beta$) of Layer 21 from 1972 (12.77 t $MJ^{-1}$ $mm^{-1}$ hr ha), which is smaller than that of Layers 1 (13.35 t $MJ^{-1}$ $mm^{-1}$ hr ha) and 2 (13.27 t $MJ^{-1}$ $mm^{-1}$ hr ha) in 1979. On the other hand, $D_m$ shows a decreasing trend from 1972 to 1979 (Fig. 9), indicating a worsening of the soil characteristics (desertification). Smaller $D_m$ values coincide with larger values of the *C* and $\beta$ factors, demonstrating that the land use types in 1979 were worse for controlling soil erosion and more susceptible to soil and water loss compared with those in 1972. Accordingly, $D_m$ can serve as a useful parameter to judge the impact of changes to land use types, which improves our understanding of layered sediments behind check dams.

### *4.2. Turning points of $D_m$*

$D_m$ is closely related to PSD according to Eqs. (3) and (4). Their close relationship is demonstrated by similar trends of $D_m$ and soil PSD of silt–clay (Fig. 11). If the PSDs of two sediment layers are the same, the $D_m$ values of the two layers are the same because $D_m$ depends on the PSDs (Eqs. (3) and (4)). However, we found that the $D_m$ of a sediment layer can be equal to another layer with different PSDs. For example, Layers 8 and 10 from the Shipanmao dam land have the same $D_m$ values, but different PSDs, and the same is true for Layer 17 from Shipanmao and Layer 4

from Zhangshan (Tables 2 and 3).

Turning points commonly exist in nature. If a time series value $X_t$ at period $t$ exceeds or is smaller than its two neighbors $X_{t-1}$ and $X_{t+1}$, $X_t$ is called a turning point (Wecker, 1979). Some values of $D_m$ and soil PSD satisfy this definition of a turning point (Fig. 11). When a $D_m$ value of the layered sediment occurs as a turning point, the corresponding soil PSD value will likely appear as a turning point as well. For example, for the Shipanmao dam land, $D_m$ in Layers 4, 11, 15, and 19 appears as turning points and so does the soil PSD in the same layers. For the Zhangshan dam land, the situation is the same for Layers 2, 8, and 11. However, the turning points of $D_m$ and PSD do not always occur synchronously. For example, $D_m$ is a turning point in Layers 3 and 5 for the Shipanmao dam land, but there are no related turning points of the PSD (Fig. 11a). The same situation can be seen for Layers 4 and 10 from the Zhangshan dam land (Fig. 11b). Comparing the layered sediments of the Shipanmao dam land with those of the Zhangshan dam land reveals that the turning points of the two dam lands are different (Fig. 11). However, the trends between two turning points of $D_m$ are the same as those of the PSD of silt–clay, and opposite to those of the PSD of fine sand (Fig. 11). This demonstrates that the factor influencing the turning points of $D_m$ is not the soil PSD of the layered sediments, but the trends of the soil PSDs in the adjacent sediment layers.

*4.3. Effect of time lag of sediment transfer on $D_m$*

The time lag of sediment delivery between the eroded soil sources and the dam land is a very complex issue. Most rainstorms on the Loess Plateau have a short duration with high intensity at a small spatial scale (Shi et al., 2012), which probably causes incomplete transfer of the eroded soils to the dam land during the rainfall events and a sediment delivery ratio (*SDR*) that is sometimes smaller than one (Zhao et al., 2015). *SDR* for the Loess Plateau is relatively high due to comparatively poor vegetation cover at various spatial scales (Jiao et al., 2014), compared with other areas such as the Murray Darling basin (70%), Australia (Lu et al., 2006), the Czech Republic (28%) (Van Rompaey et al., 2007), 61 watersheds in Spain (0.03–55%) (de Vente et al., 2008), and the Central Spanish Pyrenees (5%) (Alatorre et al., 2012). Gong and Xiong (1979) found that *SDR* was close to 1.0 in a small watershed on the Loess Plateau. Xu and Sun (2004) indicated that sediment transport was approximately equal to the gross erosion rate in the Wudinghe River basin (*SDR* = 1.0) without soil and water conservation measures. Wang et al. (2013) suggested that *SDR* was close to 1.0 for a watershed of less than 1 $km^2$ without conservation measures. Zhao et al. (2015) estimated *SDR* from a small check-dam-controlled watershed with a drainage area of 0.64 $km^2$ on the northern Loess Plateau and found that approximately 83.6% of the gross eroded soil was transported to the dam land. These studies demonstrate that *SDR* can be reduced significantly through soil and water conservation measures in watersheds. *SDR* was, for instance, reduced from 1.0 without soil and water conservation measures to 0.2–0.4 by a series of soil control measures (Xu and Sun, 2004). In this study, although the maximum flow length in the

dam-controlled area is only 1,500 m (Fig. 12), land use types such as forest, grassland, and terrace (Table 5) can serve as soil and water conservation measures according to Tang (2004). Thus, the *SDR* value in the study area should be smaller than one based on the conclusions of Gong and Xiong (1979), Xu and Sun (2004), Wang et al. (2013), and Zhao et al. (2015). However, we were unable to determine the actual *SDR* value for each storm event due to the unavailability of detailed data on the gross soil erosion caused by each storm event.

Numerous experimental results have shown that sediment becomes enriched in finer particles during the water erosion process and that the PSD of the deposited sediment is closely related to the PSD of the original soil (Moss et al., 1979; Proffitt and Rose, 1991; Shi et al., 2012). Shi et al. (2012) conducted several rainfall simulation experiments and found that the changes of PSD in the deposited sediments were small during the 54-min simulation process. The theory of erosion processes that assumes no breakdown of the soil structure during water erosion predicts that PSD at steady state will be the same as that of the original soil (Hairsine et al., 1999). Although we do not have sufficient data to verify this theory with this study, the $D_m$ of the layered sediment would remain unchanged according to Eqs. (2)–(4) only if the PSDs for both the layered sediments and the original soil were the same, regardless of the time lag of sediment transfer between soil erosion and sediment deposition. This indicates that the soil PSD is a more dominant factor affecting $D_m$ than the time lag of sediment transfer.

It is worth noting that the thickness of the 21 sediment layers in the Shipanmao dam land is 6.28 m, which has increased the dam land's altitude from 1080.00 m a.s.l. in 1972 to 1086.28 m a.s.l. in 1979 (Fig. 12). The contour line for 1086.28 m a.s.l. encloses an area of 4957 $m^2$, which accounts for only 0.25% of the total dam-controlled area of the Shipanmao dam. From this point of view, the influence of the elevation increase on sediment deposition is small at the basin scale. Accordingly, this influence was ignored in this study and the layered sediments were considered evenly distributed throughout the dam land. Soil sampling at one site of the dam land, as carried out in this study, therefore, is representative and feasible. This is different from traditional methods of soil sampling for fractal dimension analyses, which is carried out using several sampling locations (e.g., Su et al., 2004; Prosperini and Perugini, 2008). In contrast, the soil samples used in this study were collected from only one location, which is more convenient, less expensive, and less time-consuming than the traditional sampling method.

## 5. Conclusions

Soil particle size distribution (PSD) is one of the most important physical soil attributes. Fractal dimension ($D_m$) is a useful measurement to quantitatively describe soil texture, soil aggregate fragmentation, and related soil properties and has been applied widely to the field of soil science. In this study, $D_m$ was used to assess fractal characteristics of the soil PSDs of layered sediment in the dam lands of the Shipanmao and Zhangshan check dams on the Loess Plateau, and evaluate the impact

of land use types in the dam-controlled area of the Shipanmao check dam. The following conclusions are drawn.

(1) The predominant soil particle size of the layered sediments is silt–clay and fine sand, with a total percentage of more than 99.82% and 99.87% for the Shipanmao and Zhangshan dam lands, respectively. The overall gradients of the trends of silt–clay and fine sand are 0.0622 (slight increase) and −0.0618 (slight decrease), respectively, for the Shipanmao dam land, and −0.8415 (decrease) and 0.8448 (increase), respectively, for the Zhangshan dam land. There are considerable differences in PSD among the sediment layers, especially for the coarse and fine sand fractions. The coefficient of variation increases with increasing soil particle size.

(2) $D_m$ of the PSD ranges from 2.111 (Layer 11) to 2.219 (Layer 21) for the Shipanmao dam land, and from 2.144 (Layer 17) to 2.447 (Layer 2) for the Zhangshan dam land. There are several turning points of $D_m$: Layers 3, 4, 5, 11, 15, and 19 for the Shipanmao dam land, and Layers 2, 4, 8, 10, and 11 for the Zhangshan dam land. The factor influencing the turning points of $D_m$ is not the soil PSD of the layered sediments, but the trends of soil PSDs in the adjacent sediment layers.

(3) $D_m$ of the PSD for both the Shipanmao and Zhangshan dam lands has a significant positive correlation with the silt–clay size fraction, a significant negative correlation with the content of fine sand, and no correlation with the coarse sand fraction. $D_m$ decreases with the time of deposition for the Shipanmao dam land, indicating that increasing fine sand or decreasing silt–clay content can lead to a decrease in $D_m$.

(4) The land use types in the dam-controlled area of Shipanmao changed from 1972 to 1979. Compared with the land use types in 1972, sloped farmland in 1979 had a significant increase of 338,600 $m^2$; while grassland had a prominent reduction of 255,700 $m^2$. The total increment ($\Delta C_T$) of the *C* factor in 1979 was 0.021, indicating that the land use types in 1979 resulted in a positive increment of the *C* factor. The soil erosion amount per rainfall erosivity ($\beta$) was smaller in 1972 than in 1979. Smaller values for $D_m$ coincide with larger *C* and $\beta$ factors. The $D_m$ shows a decreasing trend from 1972 to 1979, indicating worsening soil conditions (desertification). The land use types prevalent in 1979 were more prone to soil and water loss compared with those in 1972. $D_m$ is a useful measure to judge the impact of land use types on dam-controlled areas of the Loess Plateau and to assess the severity of the soil desertification process.

(5) Although a time lag of sediment transfer probably exists between soil erosion and sediment deposition in the dam land, $D_m$ of layered sediment will remain unchanged only if the PSD of the layered sediment and the original soil is the same. Soil PSD is a more dominant factor affecting $D_m$ than the time lag of sediment transfer.

**Acknowledgements**

This study was supported by the National Natural Science Foundation of China (Nos. 51109103, and 41001154), and the Fundamental Research Funds for the Central Universities (Nos. lzujbky-2014-126, lzujbky-2015-149). The authors express their

appreciation to the Editor Professor Takashi Oguchi and to two anonymous reviewers for their constructive and valuable comments and suggestions.

**References**

Alatorre, L.C., Begueria, S., Lana-Renault, N., Navas, A., Garcia-Ruiz, J.M., 2012. Soil erosion and sediment delivery in a mountain catchment under scenarios of land use change using a spatially distributed numerical model. Hydrol. Earth Syst. Sc. 16(5), 1321–1334.

Boardman, J., Shepheard, M.L., Walker, E., Foster, I.D.L., 2009. Soil erosion and risk-assessment for on- and off-farm impacts: A test case using the Midhurst area, West Sussex, UK. J. Environ. Manage. 90(8), 2578–2588.

Chanson, H., 2004. Sabo check dams: Mountain protection systems in Japan. Int. J. River Basin Manage. 2(4), 301–307.

Chen, Y.Z., Jing, K., Cai, Q.G., 1988. Modern Soil Erosion and Management on the Loess Plateau, China. Science Press, Beijing, China (in Chinese).

Coppens, M., Kato, T., 1997. The Weierstrass gap sequence at an inflection point on a nodal plane curve, aligned inflection points on plane curves. B. Unione Mat. Ital. 11B(1), 1–33.

Creamer, K.M., McCloud, L.L., Fisher, L.E., Ehrhart, I.C., 1997. PEEP determined by the inflation inflection point causes overdistension. Pediatrics 100(3), 454–454.

de Vente, J., Poesen, J., Verstraeten, G., Van Rompaey, A., Govers, G., 2008. Spatially

distributed modelling of soil erosion and sediment yield at regional scales in Spain. Global Planet. Change 60(3–4), 393–415.

du Plessis, A., Harmse, T., Ahmed, F., 2015. Predicting water quality associated with land cover change in the Grootdraai Dam catchment, South Africa. Water Int. 40(4), 647–663.

Fang, R.Y., 1996. Consideration on check-dam system agriculture in Shanxi Province. Water Conserv. China (7), 47–49 (in Chinese with English abstract).

Fang, X.M., Wan, Z.Z., Kuang, S.F., 1998. Mechanism and effect of silt-arrest dams for sediment reduction in the middle Yellow River basin. J. Hydraul. Eng. 20(10), 49–53 (in Chinese with English abstract).

Feng, X.M., Wang, Y.F., Chen, L.D., Fu, B.J., Bai, G.S., 2010. Modeling soil erosion and its response to land-use change in hilly catchments of the Chinese Loess Plateau. Geomorphology 118(3–4), 239–248.

Foncin, J.F., 1996. Forced vital capacity deterioration in amyotrophic lateral sclerosis has an inflexion point - Comment. Eur. J. Neurol. 3(6), 613–613.

Fu, B.J., Liu, Y., Lu, Y.H., He, C.S., Zeng, Y., Wu, B.F., 2011. Assessing the soil erosion control service of ecosystems change in the Loess Plateau of China. Ecol. Complex. 8(4), 284–293.

Gong, S.C., Xiong, G.S., 1979. Sediment sources and spatial distribution of the Yellow River. Yellow River (1), 7–9 (in Chinese with English abstract).

Hairsine, P.B., Sander, G.C., Rose, C.W., Parlange, J.Y., Hogarth, W.L., Lisle, I., Rouhipour, H., 1999. Unsteady soil erosion due to rainfall impact: A model of

sediment sorting on the hillslope. J. Hydrol. 220(3–4), 115–128.

He, X.B., Tang, K.L., Zhang, X.C., 2004. Soil erosion dynamics on the Chinese Loess Plateau in the last 10,000 years. Mt. Res. Develop. 24(4), 342–347.

Hillel, D., 1980. Fundamentals of Soil Physics. Academic Press, New York.

Hsieh, H.M., Luo, C.R., Yang, J.C., Chen, R.F., 2013. Numerical study of the effects of check dams on erosion and sedimentation in the Pachang River. Int. J. Sediment Res. 28(3), 304–315.

Hu, J.J., Niu, P., Cao, W., 2002. Representation on the function of siltation dam engineering in the upper and middle Yellow River. J. Northwest Water Res. Water Eng. 13(2), 28–31 (in Chinese with English abstract).

Hudson, N., 1981. Soil conservation. Cornell University Press, Ithaca, N.Y.

Jebari, S., Berndtsson, R., Olsson, J., Bahri, A., 2012. Soil erosion estimation based on rainfall disaggregation. J. Hydrol. 436, 102–110.

Jiao, J.Y., Wang, W.Z., Li, J., Zheng, B.M., 2001. Soil and water conservation benef it of warping dams in hilly and gully regions on the loess plateau. J. Arid Land Resour. Environ. 15(1), 78–83 (in Chinese with English abstract).

Jiao, J.Y., Wang, W.Z., Li, J., Zheng, B.M., 2003. Silting land and sediment blocking benefit of check dam in hilly and gully region on the Loess Plateau. Trans. CSAE 19(6), 302–306 (in Chinese with English abstract).

Jiao, J.Y., Wang, Z.J., Zhao, G.J., Wang, W.Z., Mu, X.M., 2014. Changes in sediment discharge in a sediment-rich region of the Yellow River from 1955 to 2010: implications for further soil erosion control. J. Arid Land 6(5), 540–549.

Katz, A.J., Thompson, A.H., 1985. Fractal sandstone pores - implications for conductivity and pore formation. Phys. Rev. Lett. 54(12), 1325–1328.

Kefi, M., Yoshino, K., Setiawan, Y., 2012. Assessment and mapping of soil erosion risk by water in Tunisia using time series MODIS data. Paddy Water Environ. 10(1), 59–73.

Kinnell, P.I.A., 2005. Why the universal soil loss equation and the revised version of it do not predict event erosion well. Hydrol. Process. 19(3), 851–854.

Laflen, J.M., Moldenhauer, W.C., 2003. Pioneering Soil Erosion Prediction: The USLE Story. Special Publication No. 1. World Association of Soil and Water Conservation (WASWC), Beijing, China.

Lantican, M.A., Guerra, L.C., Bhuiyan, S.I., 2003. Impacts of soil erosion in the upper Manupali watershed on irrigated lowlands in the Philippines. Paddy Water Environ. 1(1), 19–26.

Li, M., 2003. Study effect of check dam on soil and water loss in the middle Yellow River. Yellow River 25(12), 25–27 (in Chinese with English abstract).

Li, X.G., Li, Z.B., Wei, X., 2007. Two key physical characteristics indexes of farmland sediment for check dams in Loess Plateau. Res. Soil Water Conserv. 14(2), 218–220, 223 (in Chinese with English abstract).

Li, X.G., Wei, X., 2011. Soil erosion analysis of human influence on the controlled basin system of check dams in small watersheds of the Loess Plateau, China. Expert Syst. Appl. 38(4), 4228–4233.

Li, X.G., Wei, X., 2014. Analysis of the relationship between soil erosion risk and

surplus floodwater during flood season. J. Hydrol. Eng. 19(7), 1294–1311.

Li, X.G., Wei, X., Wang, N.A., Cheng, H.Y., 2011. Maximum grade approach to surplus floodwater of hyperconcentration rivers in flood season and its application. Water Resour. Manag. 25(10), 2575–2593.

Lin, D.Y., 2002. Soil Science. China Forestry Publishing House, Beijing, China (in Chinese).

Liu, X., Zhang, G.C., Heathman, G.C., Wang, Y.Q., Huang, C.H., 2009. Fractal features of soil particle-size distribution as affected by plant communities in the forested region of Mountain Yimeng, China. Geoderma 154(1–2), 123–130.

Liu, Y., Fu, B.J., Lu, Y.H., Wang, Z., Gao, G.Y., 2012. Hydrological responses and soil erosion potential of abandoned cropland in the Loess Plateau, China. Geomorphology 138(1), 404–414.

Lobe, I., Amelung, W., Du Preez, C.C., 2001. Losses of carbon and nitrogen with prolonged arable cropping from sandy soils of the South African Highveld. Eur. J. Soil Sci. 52(1), 93–101.

Lu, H., Moran, C.J., Prosser, I.P., 2006. Modelling sediment delivery ratio over the Murray Darling Basin. Environ. Modell. Softw. 21(9), 1297–1308.

Lu, Y.H., Sun, R.H., Fu, B.J., Wang, Y.F., 2012. Carbon retention by check dams: Regional scale estimation. Ecol. Eng. 44, 139–146.

Magiera, A., 1997. Point of inflection in the coherent two-photon fluorescent microscope of annular pupil. Opt. Appl. 27(4), 291–298.

Mandelbrot, B.B., 1982. The fractal geometry of nature. W.H. Freeman, San Francisco.

Marques, M.J., Bienes, R., Perez-Rodriguez, R., Jimenez, L., 2008. Soil degradation in Central Spain due to sheet water erosion by low-intensity rainfall events. Earth Surf. Proc. Land. 33(3), 414–423.

MartiFabregas, J., 1996. Forced vital capacity deterioration in amyotrophic lateral sclerosis has an inflexion point - Reply. Eur. J. Neurol. 3(6), 614–614.

Meng, Q.M., 1996. Soil and Water Conservation in the Chinese Loess Plateau. Yellow River Conservancy Press, Zhengzhou, China (in Chinese).

Moss, A.J., Walker, P.H., Hutka, J., 1979. Raindrop-stimulated transportation in shallow water flows: An experimental study. Sedimentary Geology 22(3–4), 165–184.

MWR (Ministry of Water Resources of China), 2002. The Bulletin of Soil and Water Loss of China, Beijing, China (in Chinese).

Ni, J.R., Li, X.X., Borthwick, A.G.L., 2008. Soil erosion assessment based on minimum polygons in the Yellow River basin, China. Geomorphology 93(3–4), 233–252.

Ozcan, A.U., Erpul, G., Basaran, M., Erdogan, H.E., 2008. Use of USLE/GIS technology integrated with geostatistics to assess soil erosion risk in different land uses of Indagi Mountain Pass-Cankiri, Turkey. Environ. Geol. 53(8), 1731–1741.

Pachepsky, Y.A., Polubesova, T.A., Hajnos, M., Sokolowska, Z., Jozefaciuk, G., 1995.

Fractal parameters of pore surface-area as influenced by simulated soil degradation. Soil Sci. Soc. Am. J. 59(1), 68–75.

Perfect, E., 1997. Fractal models for the fragmentation of rocks and soils: A review. Eng. Geol. 48(3–4), 185–198.

Perfect, E., Kay, B.D., 1995. Applications of fractals in soil and tillage research: A review. Soil Till. Res. 36(1–2), 1–20.

Pimentel, D., Kounang, N., 1998. Ecology of soil erosion in ecosystems. Ecosystems 1(5), 416–426.

Proffitt, A.P.B., Rose, C.W., 1991. Soil erosion processes .II. Settling velocity characteristics of eroded sediment. Aust. J. Soil Res. 29(5), 685–695.

Prosperini, N., Perugini, D., 2007. Application of a cellular automata model to the study of soil particle size distributions. Physica A 383(2), 595–602.

Prosperini, N., Perugini, D., 2008. Particle size distributions of some soils from the Umbria Region (Italy): Fractal analysis and numerical modelling. Geoderma 145(3–4), 185–195.

Ran, D.C., Luo, Q.H., Liu, B., Wang, H.J., 2004. Effect of soil-retaining dams on flood and sediment reduction in middle reaches of Yellow River. J. Hydraul. Eng. (5), 7–13 (in Chinese with English abstract).

Ran, D.C., Luo, Q.H., Zhou, Z.H., Wang, G.Q., Zhang, X.H., 2008. Sediment retention by check dams in the Hekouzhen-Longmen section of the Yellow River. Int. J. Sediment Res. 23(2), 159–166.

Rapp, J.F., Lopes, V.L., Renard, K.G., 2001. Comparing soil erosion estimates from

RUSLE and USLE on natural runoff plots. In: J.C. AscoughII II, D.C. Flanagan (Eds.), Proceedings of International Symposium of Soil Erosion Research for the 21st Century. American Society Agricultural Engineers, Honolulu, HI, USA, pp. 24–27.

Ren, M.E., Shi, Y.L., 1986. Sediment discharge of the Yellow-River (China) and its effect on the sedimentation of the Bohai and the Yellow Sea. Cont. Shelf Res. 6(6), 785–810.

Risse, L.M., Nearing, M.A., Nicks, A.D., Laflen, J.M., 1993. Error assessment in the Universal Soil Loss Equation. Soil Sci. Soc. Am. J. 57(3), 825–833.

Romero-Diaz, A., Marin-Sanleandro, P., Ortiz-Silla, R., 2012. Loss of soil fertility estimated from sediment trapped in check dams. South-eastern Spain. Catena 99, 42–53.

Shi, H., Shao, M.A., 2000. Soil and water loss from the Loess Plateau in China. J. Arid Environ. 45(1), 9–20.

Shi, Z.H., Fang, N.F., Wu, F.Z., Wang, L., Yue, B.J., Wu, G.L., 2012. Soil erosion processes and sediment sorting associated with transport mechanisms on steep slopes. J. Hydrol. 454–455, 123–130.

Shrestha, D.P., Yazidhi, B., Teklehaimanot, G., 2004. Assessing soil losses using erosion models and terrain parameters: a case study in Thailand, Proceedings of the 25th Asian Conference on Remote Sensing, 2004 Silver Jubilee. Geo-Informatics and Space Technology Development Agency (GISTDA), Chiang Mai, Thailand, pp. 1093–1098.

Su, Y.Z., Zhao, H.L., 2003. Losses of soil organic carbon and nitrogen and their mechanisms in the desertification process of sandy farmlands in Horqin Sandy Land. Agr. Sci. China 2(7), 890–897.

Su, Y.Z., Zhao, H.L., Zhao, W.Z., Zhang, T.H., 2004. Fractal features of soil particle size distribution and the implication for indicating desertification. Geoderma 122(1), 43–49.

Suri, M., Cebecauer, T., Hofierka, J., Fulajtar, E., 2002. Soil erosion assessment of Slovakia at a regional scale using GIS. Ecology (Bratislava) 21(4), 404–422.

SWCB (Soil and Water Conservation Bureau SWCB of the Yellow River Conservancy Commission of the Chinese Ministry of Water Resources), 2003. Practice and Exploration of Check-Dam System for Small Watersheds in the Yellow River Basin. Yellow River Conservancy Commission of the Chinese Ministry of Water Resources, Zhengzhou, China (in Chinese).

Sylvain, J.M., Assani, A., Landry, R., Quessy, J.F., Kinnard, C., 2015. Comparison of the spatio-temporal variability of annual minimum daily extreme flow characteristics as a function of land use and dam management mode in Quebec, Canada. Water 7(3), 1232–1245.

Tang, K.L., 2004. Soil and Water Conservation in China. China Science Press, Beijing, China (in Chinese).

Turcotte, D.L., 1986. Fractals and fragmentation. J. Geophys. Res.-Solid 91(B2), 1921–1926.

Tyler, S.W., Wheatcraft, S.W., 1992. Fractal scaling of soil particle-size distributions -

Analysis and limitations. Soil Sci. Soc. Am. J. 56(2), 362–369.

UMYRBYRCC (Upper and Middle Yellow River Bureau of Yellow River Conservancy Commission), 2000. Effects Analysis on Water and Sediment Reduction of Soil and Water Conservation Measures in Jinghe River Basin, Xifeng, Gansu Province, China (in Chinese).

Valentin, C., Poesen, J., Li, Y., 2005. Gully erosion: impacts, factors and control. Catena 63(2–3), 132–153.

Van Rompaey, A., Krasa, J., Dostal, T., 2007. Modelling the impact of land cover changes in the Czech Republic on sediment delivery. Land Use Policy 24(3), 576–583.

Wang, D., Fu, B.J., Zhao, W.W., Hu, H.F., Wang, Y.F., 2008. Multifractal characteristics of soil particle size distribution under different land-use types on the Loess Plateau, China. Catena 72(1), 29–36.

Wang, Z.J., Ma, L.M., Jiao, J.Y., 2013. Sediment delivery ratio in different spatial scale watershed in Loess Hilly-gully region. Soil Water Conserv. (6), 1–8 (in Chinese with English abstract).

Wecker, W.E., 1979. Predicting the turning points of a time series. J. Business 52(1), 35–50.

Wei, X., Li, Z.B., Li, X.G., Lu, K.X., 2006a. Distribution law of deposits' dry bulk density and its application in sediment restoration of check dam. J. Northwest Sci-Tech Univ. Agr. For. (Nat. Sci. Ed.) 34(10), 192–196 (in Chinese with English abstract).

Wei, X., Li, Z.B., Shen, B., Li, X.G., Lu, K., 2006b. Depositing process of check dams on loess plateau in Northern Shaanxi Province. Trans. CSAE 22(9), 80–84 (in Chinese with English abstract).

Wischmeier, W.H., Smith, D.D., 1958. Rainfall energy and its relationship to soil loss. Trans. AGU 39(2), 285–291.

Wischmeier, W.H., Smith, D.D., 1965. Predicting rainfall erosion losses from cropland east of the Rocky Mountains. Agricultural Handbook No.282, Purdue Agricultural Experiment station, West Lafayette, Indiana, USA.

Wischmeier, W.H., Smith, D.D., 1978. Predicting rainfall erosion losses -a guide to conservation planning with the universal soil loss equation (USLE). Agriculture Handbook No.537, Springfield, USA.

Wu, Q., Wang, M.Y., 2007. A framework for risk assessment on soil erosion by water using an integrated and systematic approach. J. Hydrol. 337(1–2), 11–21.

Xia, D., Deng, Y.S., Wang, S.L., Ding, S.W., Cai, C.F., 2015. Fractal features of soil particle-size distribution of different weathering profiles of the collapsing gullies in the hilly granitic region, south China. Nat. Hazards 79(1), 455–478.

Xu, G.C., Li, Z.B., Li, P., 2013. Fractal features of soil particle-size distribution and total soil nitrogen distribution in a typical watershed in the source area of the middle Dan River, China. Catena 101, 17–23.

Xu, J.X., 1998. A study of physico-geographical factors for formation of hyperconcentrated flows in the Loess Plateau of China. Geomorphology 24(2–3), 245–255.

Xu, J.X., 2003. Sediment flux to the sea as influenced by changing human activities and precipitation: Example of the Yellow River, China. Environ. Manage. 31(3), 328–341.

Xu, J.X., Sun, J., 2004. Effect of erosion control measure on sediment delivery ratio. Adv. Water Sci. 15(1), 29–34 (in Chinese with English abstract).

Xu, J.X., Sun, J., 2006. Study of temporal variation of check dam construction in Wudinghe River Basin and some suggestion for some countermeasure. J. Soil Water Conserv. 20(2), 26–30 (in Chinese with English abstract).

Xu, X.Z., Zhang, H.W., Wang, G.Q., Peng, Y., Zhang, O.Y., 2006. A laboratory study on the relative stability of the check-dam system in the Loess Plateau, China. Land Degrad. Dev. 17(6), 629–644.

Yin, S., Xie, Y., Nearing, M.A., Wang, C., 2007. Estimation of rainfall erosivity using 5-to 60-minute fixed-interval rainfall data from China. Catena 70(3), 306–312.

Yu, J.B., Lv, X.F., Bin, M., Wu, H.F., Du, S.Y., Zhou, M., Yang, Y.M., Han, G.X., 2015. Soil erosion processes and sediment sorting associated with. Sci. Rep. 5, 1–9.

Zalibekov, Z.G., 2002. Changes in the soil cover as a result of desertification. Eurasian Soil Sci. 35(12), 1276–1281.

Zeng, Q.L., Yue, Z.Q., Yang, Z.F., Zhang, X.J., 2009. A case study of long-term field performance of check-dams in mitigation of soil erosion in Jiangjia stream, China. Environ. Geol. 58(4), 897–911.

Zhang, X., Quine, T.A., Walling, D.E., 1998. Soil erosion rates on sloping cultivated

land on the Loess Plateau near Ansai, Shaanxi Province, China: An investigation using Cs-137 and rill measurements. Hydrol. Process. 12(1), 171–189.

Zhang, X.B., Wen, Z.M., Feng, M.Y., Yang, Q.K., Zhang, J.J., 2007. Application of (CS)-C-137 fingerprinting technique to interpreting sediment production records from reservoir deposits in a small catchment of the Hilly Loess Plateau, China. Sci. China Ser. D 50(2), 254–260.

Zhao, G.J., Klik, A., Mu, X.M., Wang, F., Gao, P., Sun, W.Y., 2015. Sediment yield estimation in a small watershed on the northern Loess Plateau, China. Geomorphology 241, 343–352.

Zhao, P.P., Shao, M.A., Melegy, A.A., 2010a. Soil water distribution and movement in layered soils of a dam farmland. Water Resour. Manag. 24(14), 3871–3883.

Zhao, P.P., Shao, M.A., Wang, T.J., 2010b. Spatial distributions of soil surface-layer saturated hydraulic conductivity and controlling factors on dam farmlands. Water Resour. Manag. 24(10), 2247–2266.

Zheng, F.L., 2006. Effect of vegetation changes on soil erosion on the Loess Plateau. Pedosphere 16(4), 420–427.

Zheng, M.G., Cai, Q.G., Cheng, Q.J., 2008. Modelling the runoff-sediment yield relationship using a proportional function in hilly areas of the Loess Plateau, North China. Geomorphology 93(3–4), 288–301.

Zhou, P., Luukkanen, O., Tokola, T., Nieminen, J., 2008. Effect of vegetation cover on soil erosion in a mountainous watershed. Catena 75(3), 319–325.

**Figure captions**

Fig.1. Locations of the Xiaohegou and Hongheze watersheds and the Shipanmao and Zhangshan check dams.

Fig. 2. Average precipitation and temperature at Caoping station: (a) annual and (b) monthly variability during 1972–1979.

Fig. 3. Layered sediments from the Shipanmao dam land.

Fig. 4. Changing characteristics of the soil PSD for silt–clay (< 0.05 mm) and fine sand (0.25–0.05 mm) for the (a) Shipanmao and (b) Zhangshan dam lands.

Fig. 5. Coefficient of variation for soil PSDs of layered sediment from the (a) Shipanmao and (b) Zhangshan dam lands.

Fig. 6. Changing trend of fractal dimension $D_m$ for the layered sediment from the Shipanmao and Zhangshan dam lands.

Fig. 7. Changing trends of fractal dimension $D_m$ between turning points for the layered sediments from the (a) Shipanmao and (b) Zhangshan dam lands.

Fig. 8. Relationships between fractal dimension and soil particle size distribution for (a) silt–clay (<0.05 mm) from Shipanmao, (b) fine sand (0.25–0.05 mm) from Shipanmao, (c) coarse sand (0.50–0.25 mm) from Shipanmao, (d) silt–clay (<0.05 mm) from Zhangshan, (e) fine sand (0.25–0.05 mm) from Zhangshan, and (f) coarse sand (1.0–0.25 mm) from Zhangshan dam lands.

Fig. 9. Changing trend of fractal dimension for the Shipanmao dam land during 1972–1979.

Fig. 10. Changing trend of soil particle size distribution for slit–clay (<0.05 mm) and fine sand (0.25–0.05 mm) from the Shipanmao dam land during 1972–1979.

Fig. 11. Trends and turning points of fractal dimension ($D_m$) (arrows) and soil particle size distributions (PSDs) for the (a) Shipanmao and (b) Zhangshan dam lands.

Fig. 12. Area surrounded by the 1086.28 m a.s.l. contour in the dam land of the Shipanmao; contour line is based on the Hydrology module of ArcGIS 10.0 (ESRI, Redlands, California).

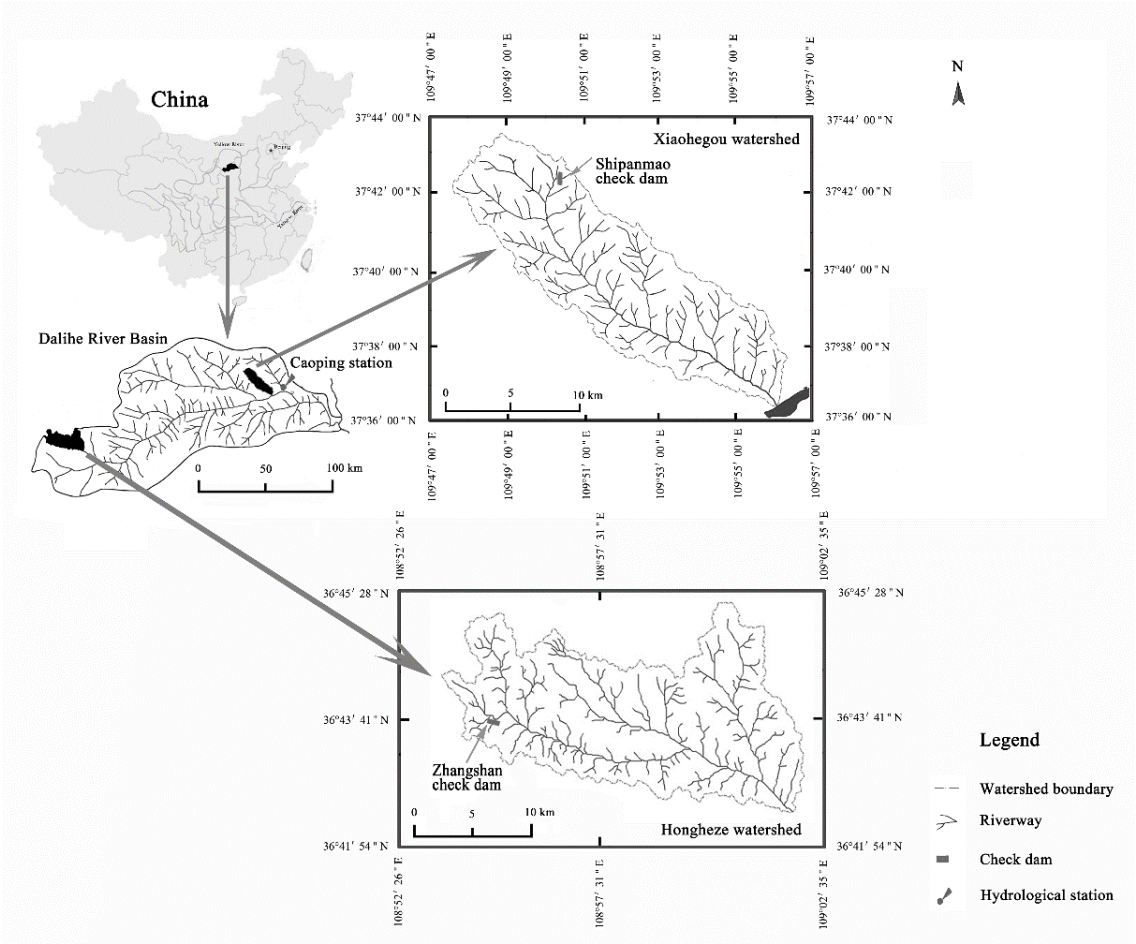


**Fig.1.**

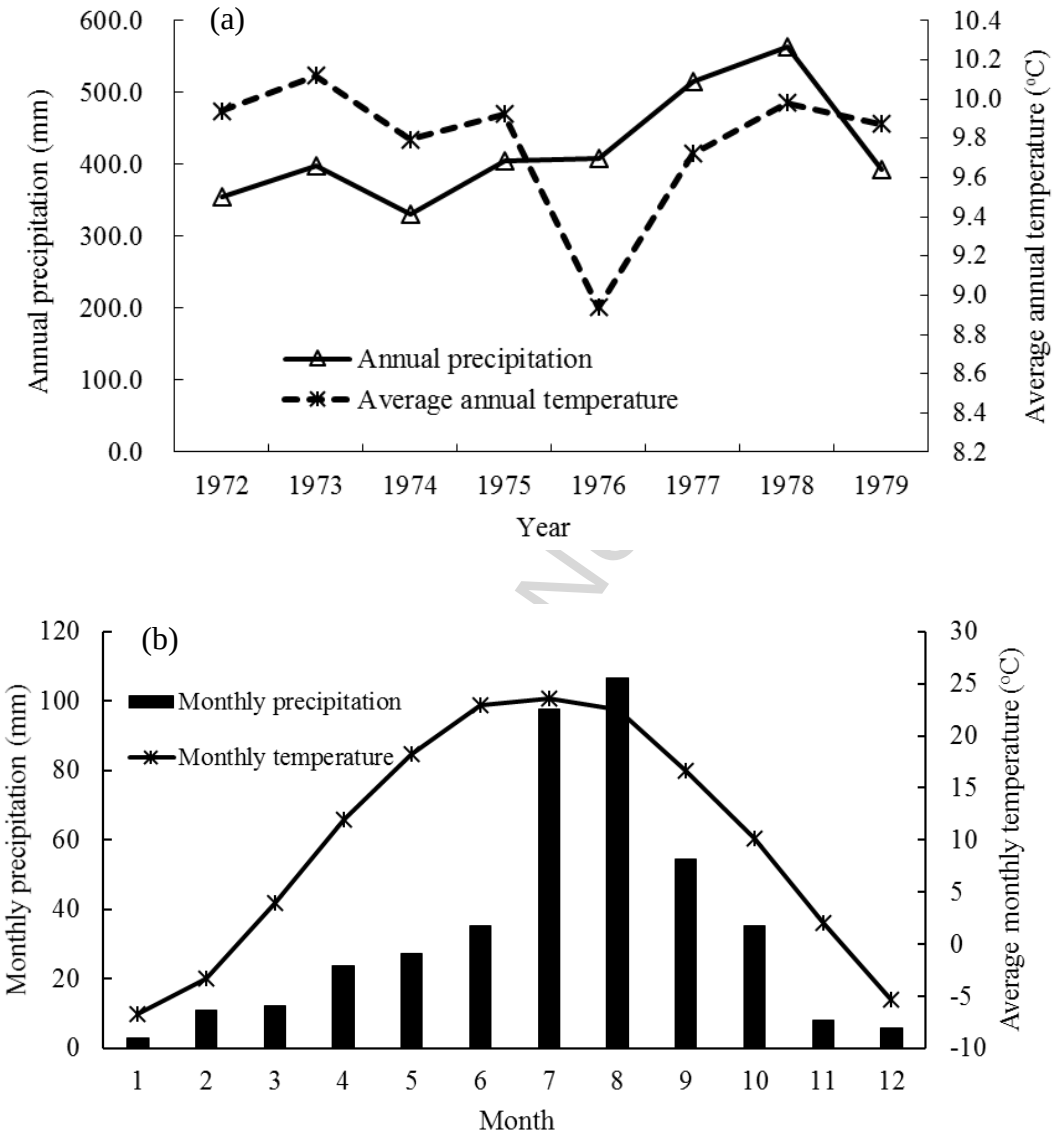


**Fig. 2.**

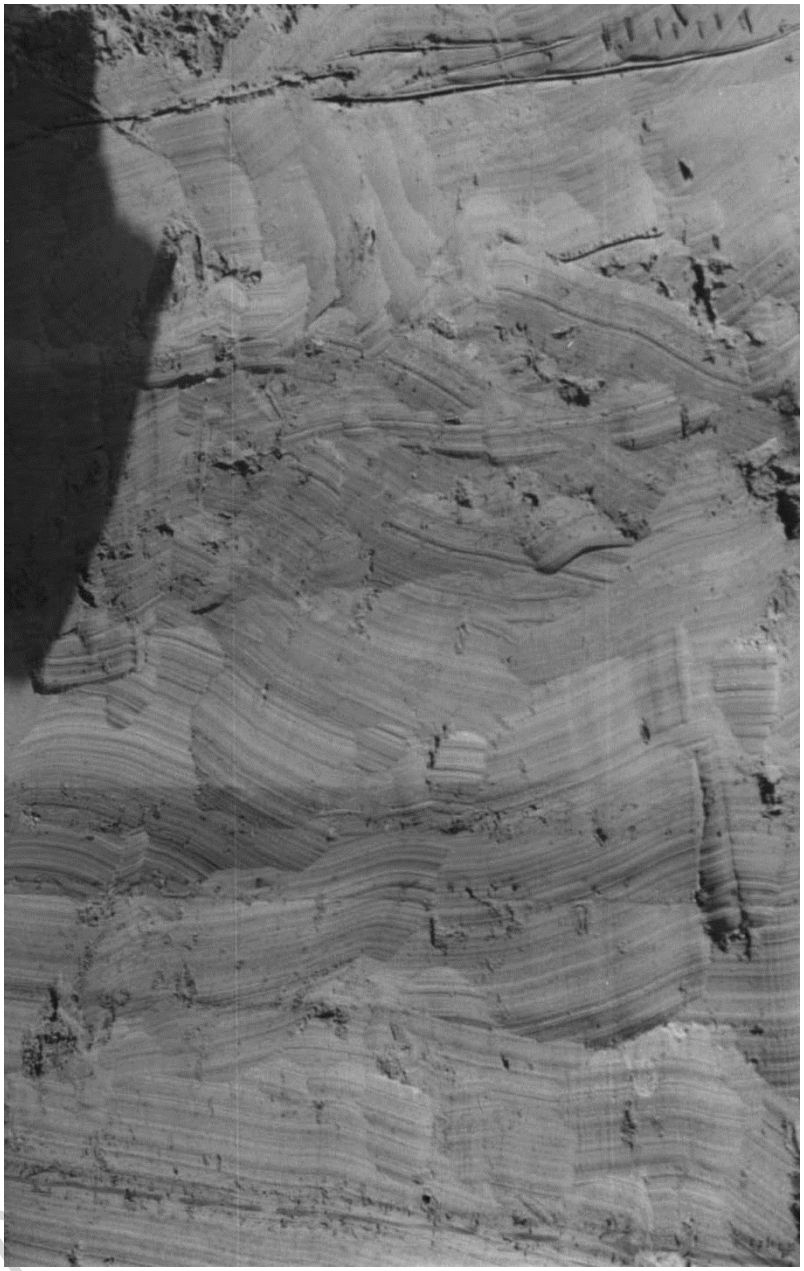

**Fig. 3.**

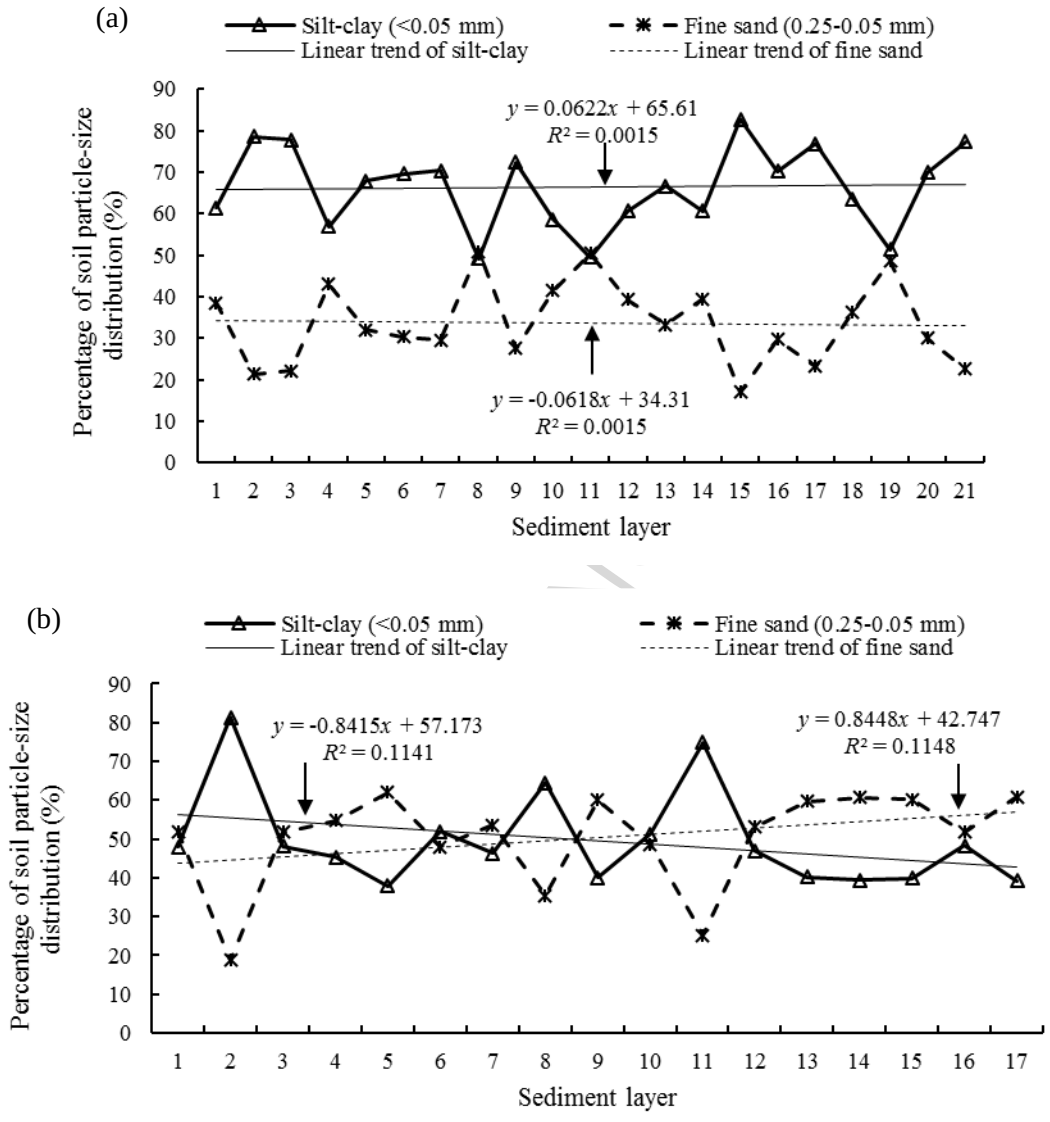


**Fig. 4**

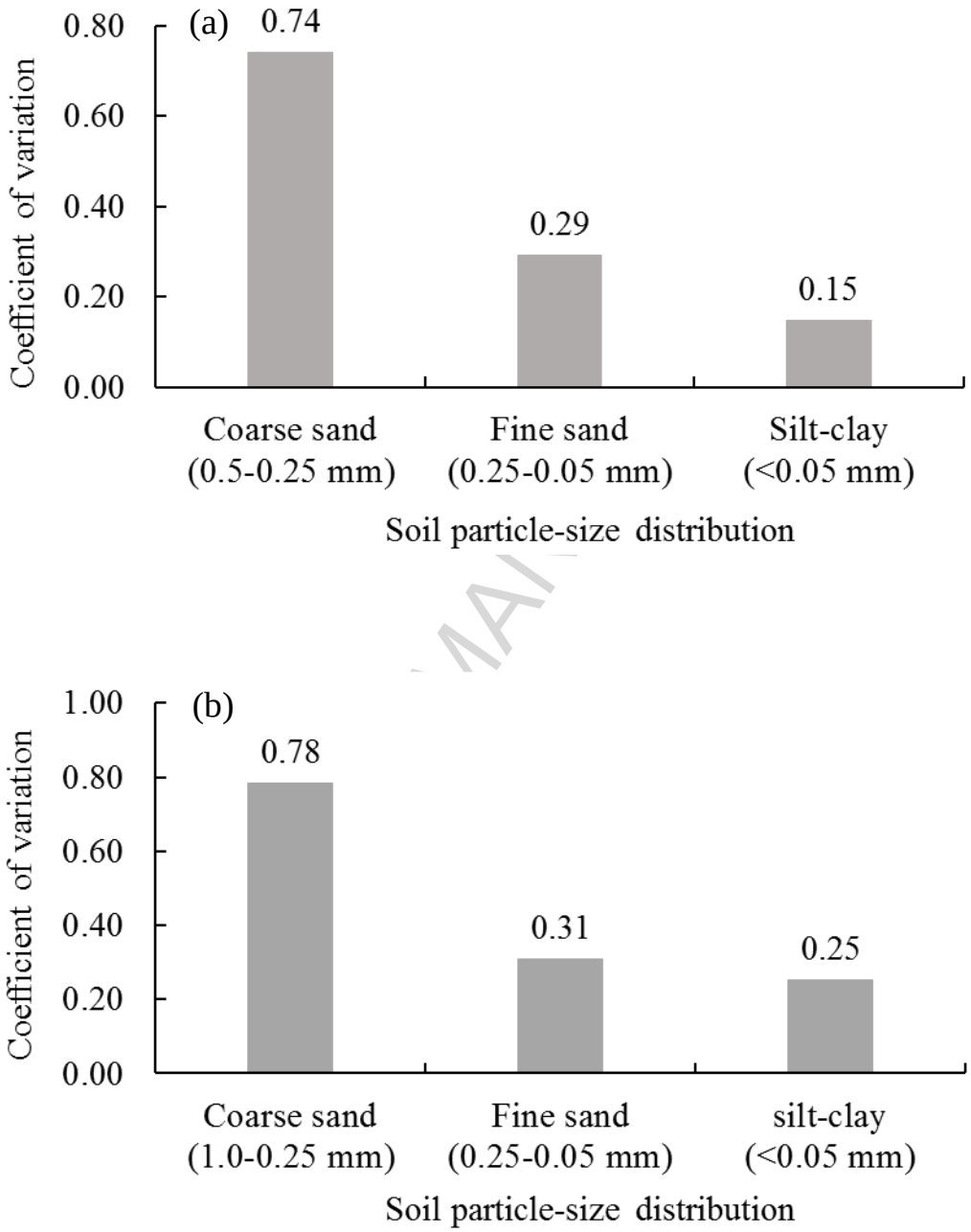


**Fig. 5.**

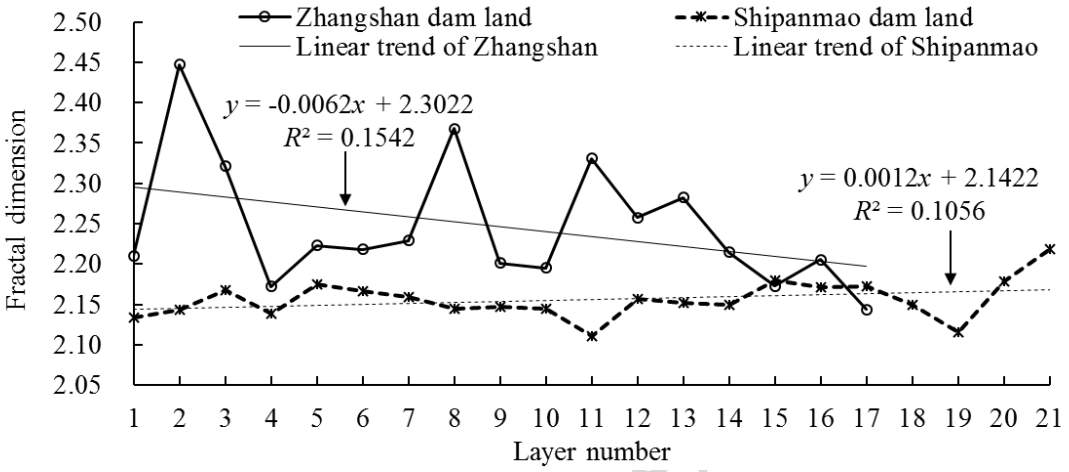


**Fig. 6.**

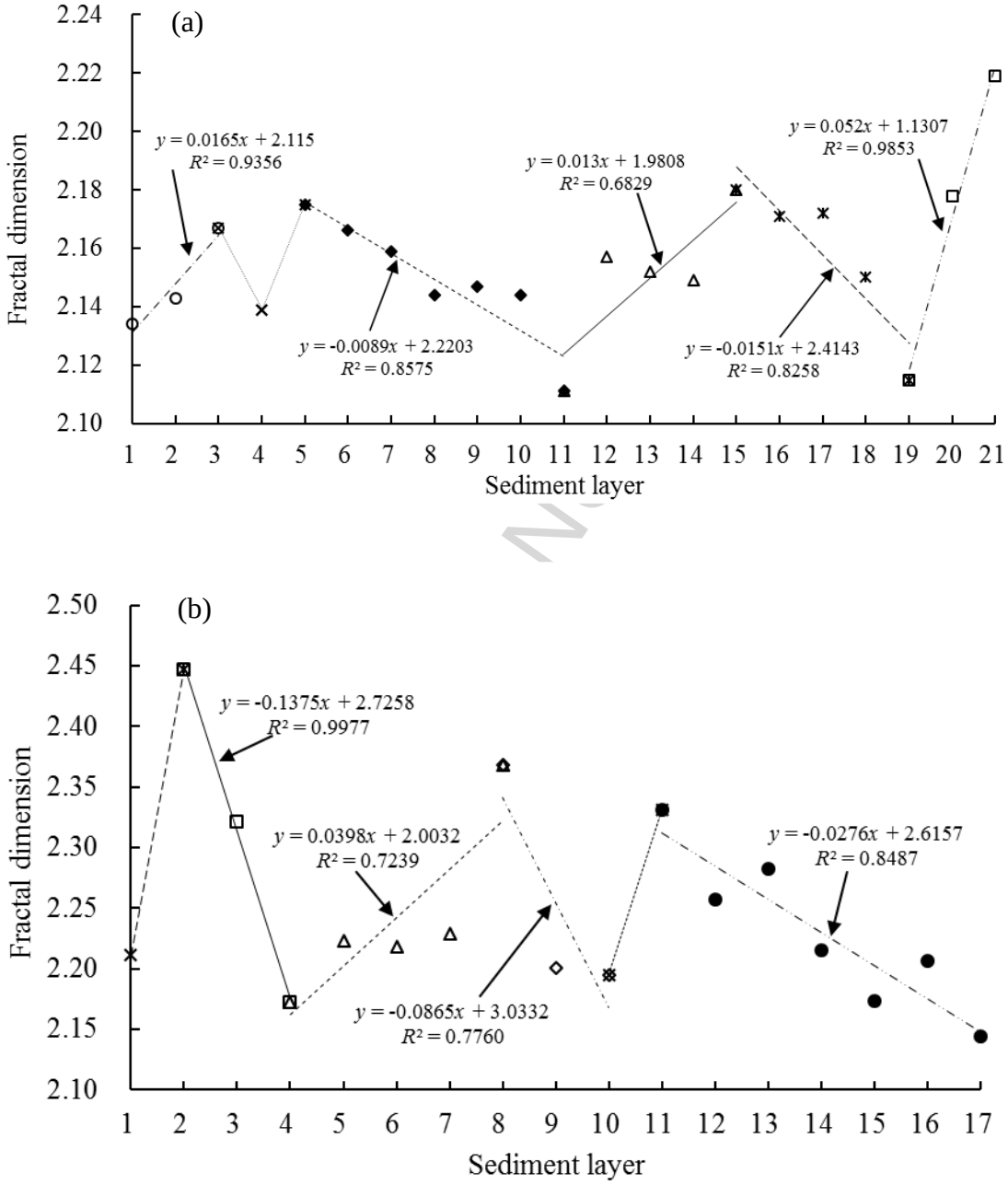


**Fig. 7.**

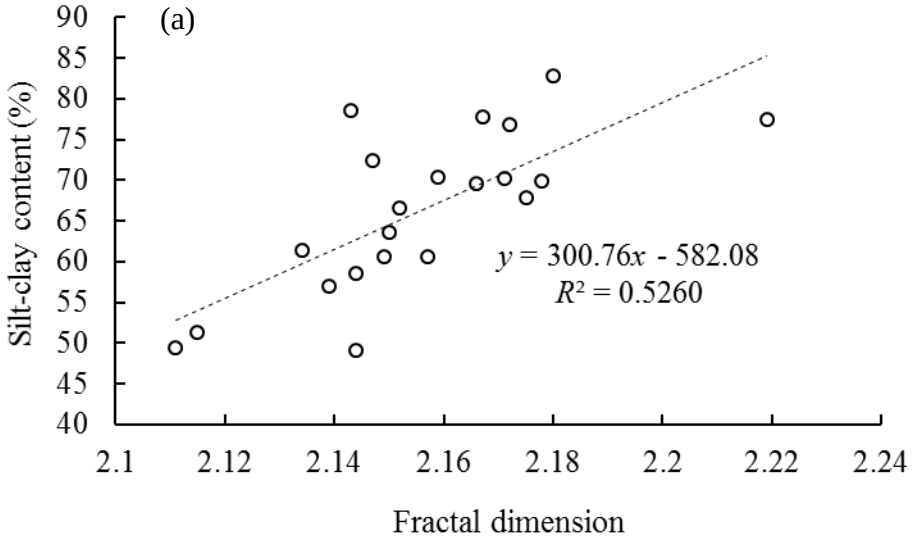


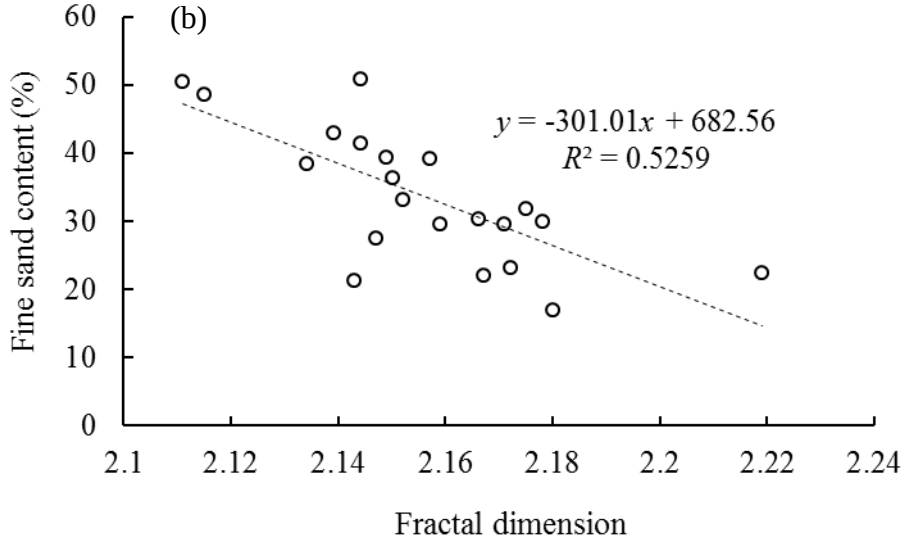


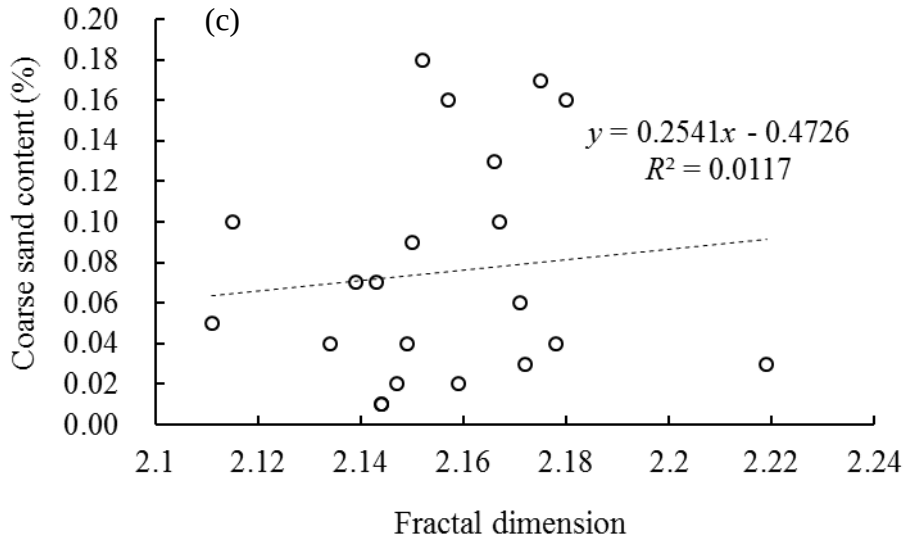

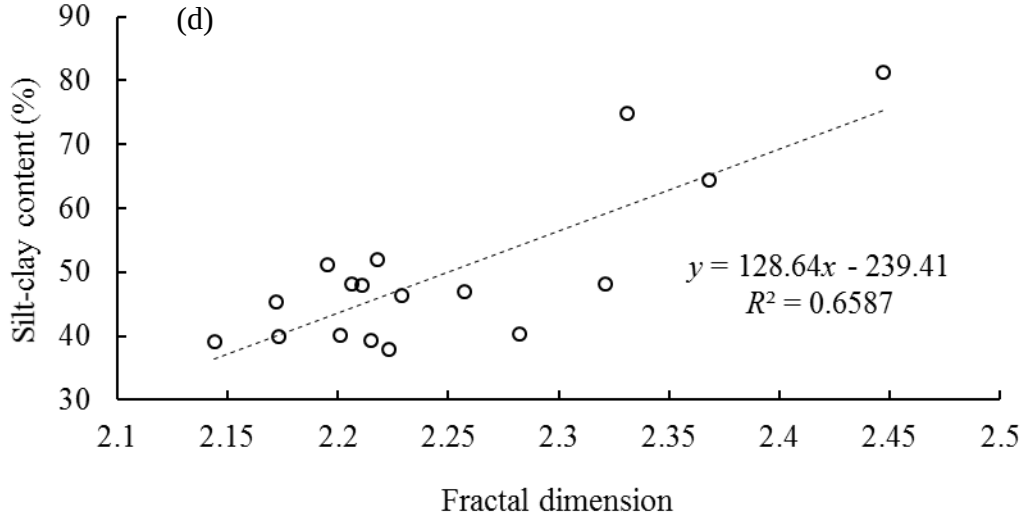


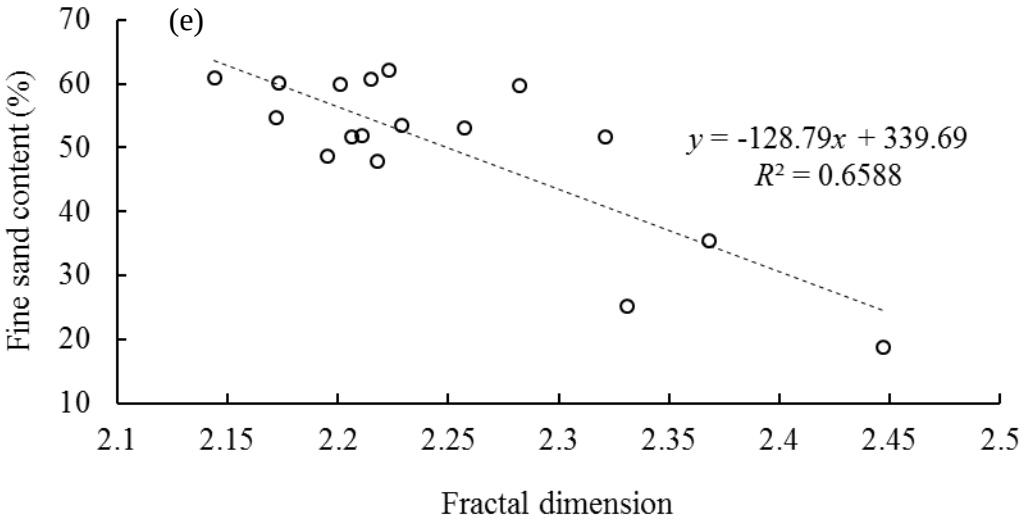


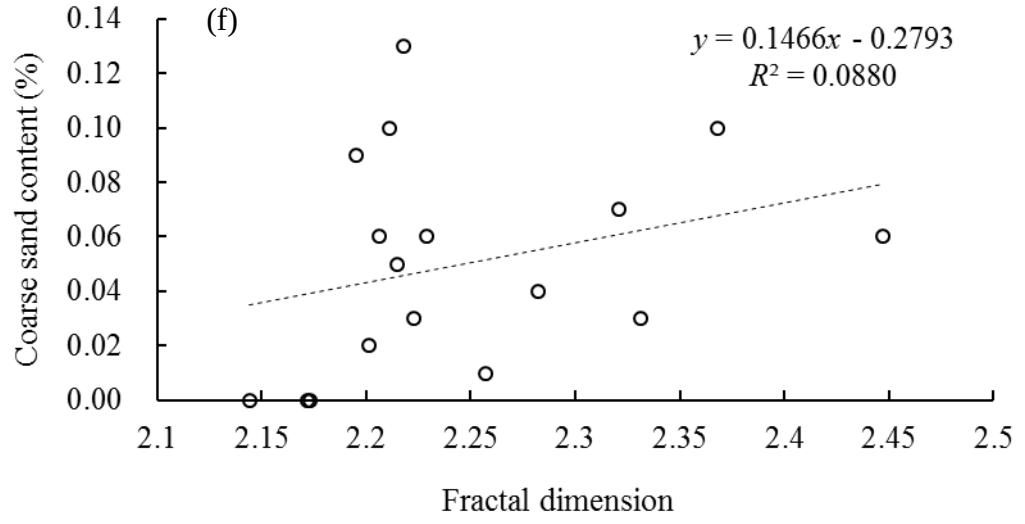

**Fig. 8.**

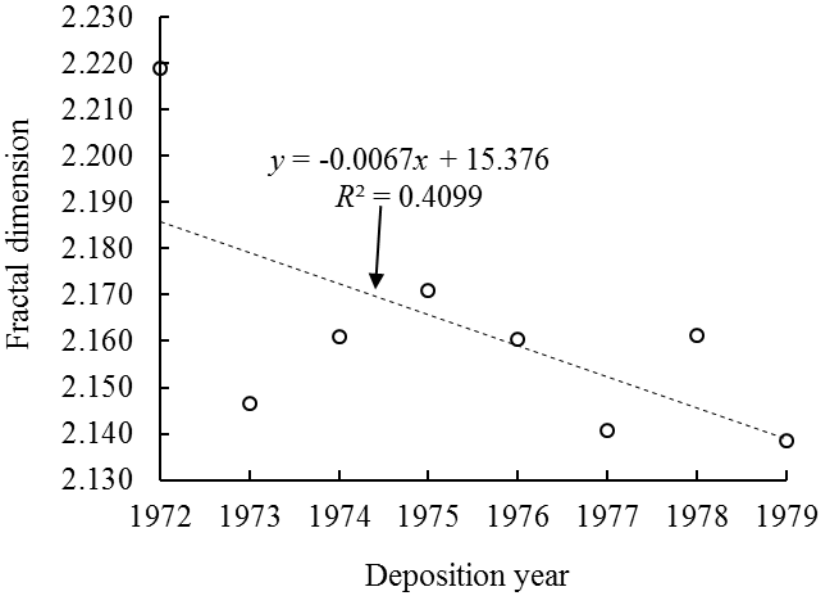


**Fig. 9.**

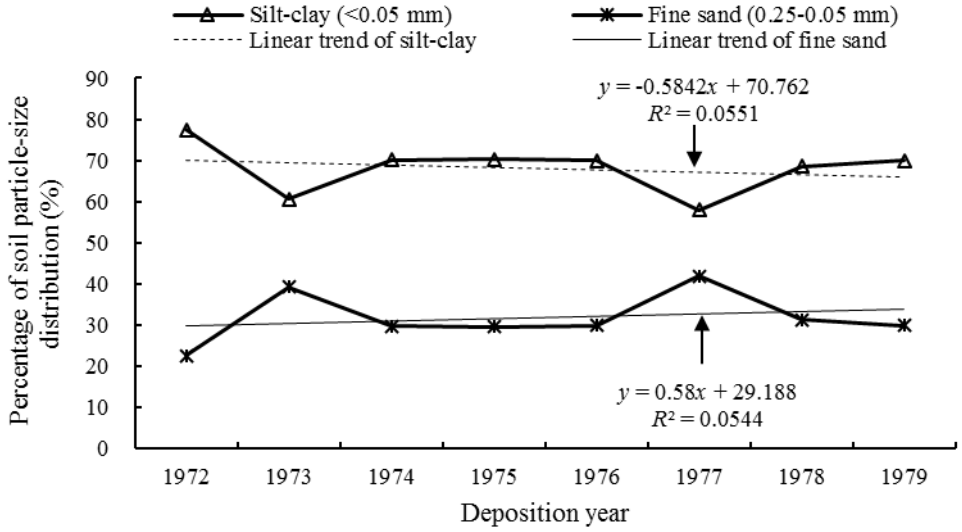


**Fig. 10.**

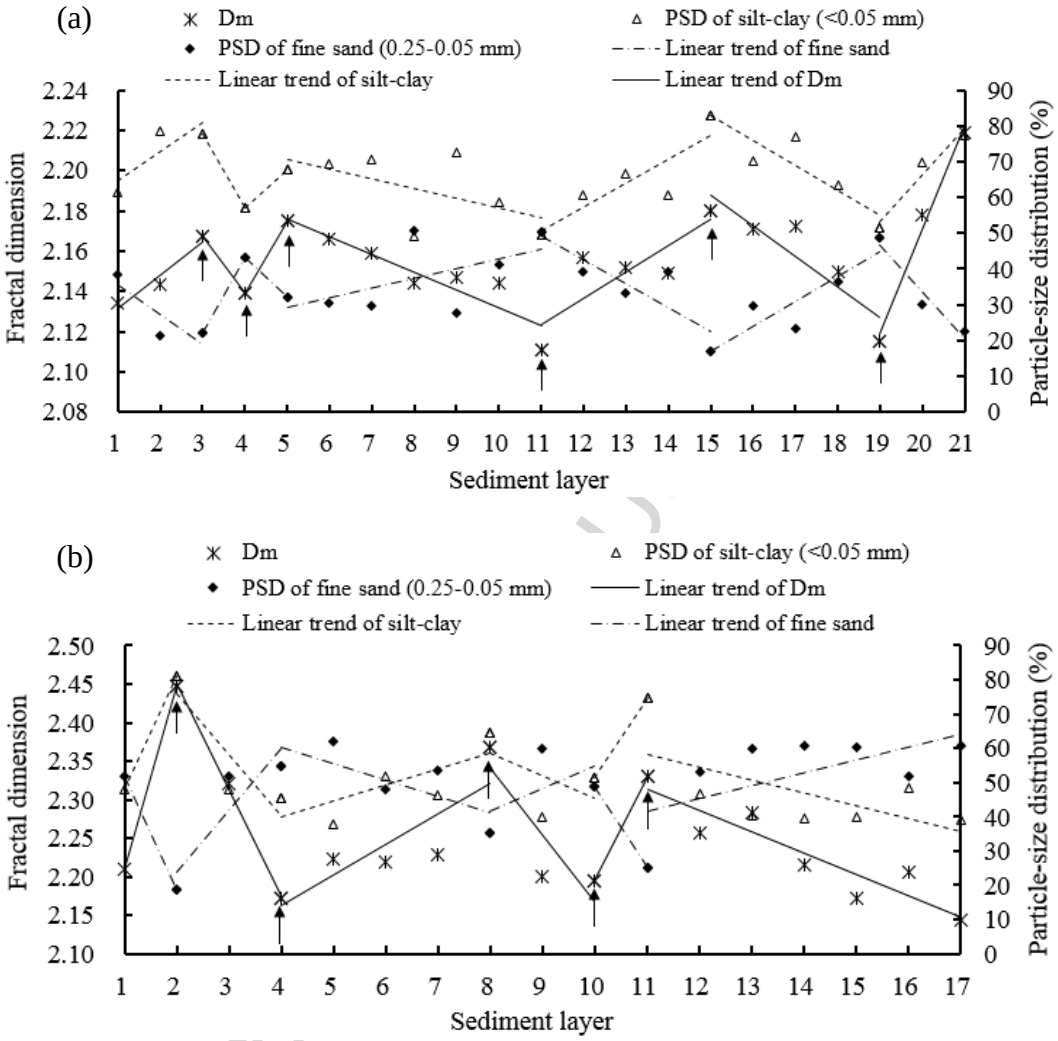


**Fig. 11.**

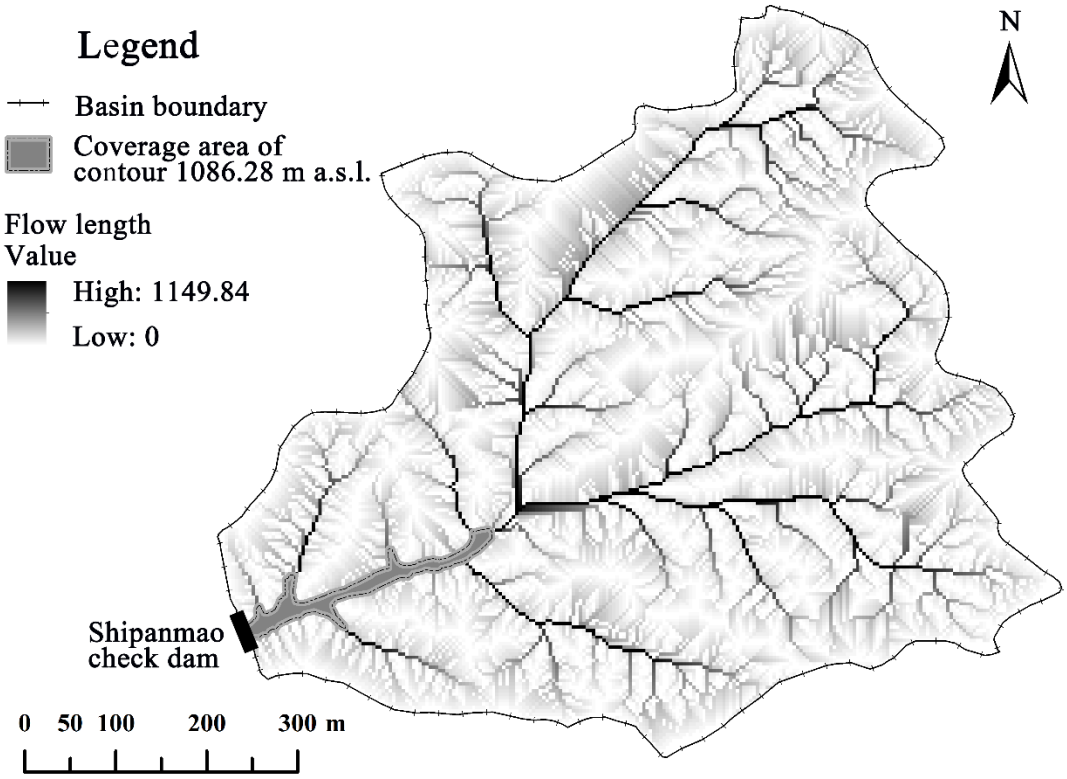


**Fig. 12**

Table 1. Link between sediment layers and rainstorm events for the Shipanmao dam land.

| Deposition year | Sediment layers |
|---|---|
| 1972 | 21 |
| 1973 | 19–20 |
| 1974 | 17–18 |
| 1975 | 16 |
| 1976 | 13–15 |
| 1977 | 8–12 |
| 1978 | 3–7 |
| 1979 | 1–2 |

Table 2. Soil particle size distribution and fractal dimension $D_m$ of layered sediment from the Shipanmao dam land.

| Sediment layer | Soil particle size distribution(mm) | | | | | | $D_m$ | Determination coefficient $R^2$ |
|---|---|---|---|---|---|---|---|---|
| | Gravel | Coarse sand | | Fine sand | | Silt–clay | | |
| | 2.0–1.0 | 1.0–0.5 | 0.5–0.25 | 0.25–0.1 | 0.1–0.05 | <0.05 | | |
| 1 | 0 | 0 | 0.04 | 4.23 | 34.27 | 61.46 | 2.134 | 0.90 |
| 2 | 0 | 0 | 0.07 | 6.38 | 15.01 | 78.54 | 2.143 | 0.87 |
| 3 | 0 | 0 | 0.10 | 3.93 | 18.18 | 77.79 | 2.167 | 0.88 |
| 4 | 0 | 0 | 0.07 | 12.52 | 30.46 | 56.95 | 2.139 | 0.89 |
| 5 | 0 | 0 | 0.17 | 3.17 | 28.77 | 67.89 | 2.175 | 0.89 |
| 6 | 0 | 0 | 0.13 | 1.89 | 28.43 | 69.55 | 2.166 | 0.89 |
| 7 | 0 | 0 | 0.02 | 8.12 | 21.42 | 70.44 | 2.159 | 0.87 |
| 8 | 0 | 0 | 0.01 | 9.43 | 41.42 | 49.14 | 2.144 | 0.90 |
| 9 | 0 | 0 | 0.02 | 9.04 | 18.51 | 72.43 | 2.147 | 0.87 |
| 10 | 0 | 0 | 0.01 | 12.80 | 28.58 | 58.61 | 2.144 | 0.89 |
| 11 | 0 | 0 | 0.05 | 10.93 | 39.56 | 49.46 | 2.111 | 0.93 |
| 12 | 0 | 0 | 0.16 | 11.42 | 27.82 | 60.6 | 2.157 | 0.88 |
| 13 | 0 | 0 | 0.18 | 9.64 | 23.55 | 66.63 | 2.152 | 0.90 |
| 14 | 0 | 0 | 0.04 | 13.59 | 25.79 | 60.58 | 2.149 | 0.88 |
| 15 | 0 | 0 | 0.16 | 6.34 | 10.69 | 82.81 | 2.180 | 0.84 |
| 16 | 0 | 0 | 0.06 | 10.00 | 19.69 | 70.25 | 2.171 | 0.86 |
| 17 | 0 | 0 | 0.03 | 6.67 | 16.49 | 76.81 | 2.172 | 0.84 |
| 18 | 0 | 0 | 0.09 | 3.86 | 32.46 | 63.59 | 2.150 | 0.93 |
| 19 | 0 | 0 | 0.10 | 24.6 | 23.96 | 51.34 | 2.115 | 0.87 |
| 20 | 0 | 0 | 0.04 | 8.13 | 21.92 | 69.91 | 2.178 | 0.86 |

| | | | | | | | | |
|---|---|---|---|---|---|---|---|---|
| 21 | 0 | 0 | 0.03 | 2.34 | 20.22 | 77.41 | 2.219 | 0.87 |

Note: layers were numbered from the top (surface soil) to the bottom (subsoil) of the dam land.

Table 3. Soil particle size distribution and fractal dimension $D_m$ of layered sediment from the Zhangshan dam land.

| Sediment layer | Soil particle size distribution (mm) | | | | | | $D_m$ | Determination coefficient $R^2$ |
|---|---|---|---|---|---|---|---|---|
| | Gravel | Coarse sand | | Fine sand | | Silt–clay | | |
| | 2.0–1.0 | 1.0–0.5 | 0.5–0.25 | 0.25–0.1 | 0.1–0.05 | <0.05 | | |
| 1 | 0 | 0 | 0.10 | 17.22 | 34.72 | 47.96 | 2.211 | 0.93 |
| 2 | 0 | 0.02 | 0.04 | 8.44 | 10.29 | 81.21 | 2.447 | 0.86 |
| 3 | 0 | 0.03 | 0.04 | 20.76 | 30.98 | 48.19 | 2.321 | 0.91 |
| 4 | 0 | 0 | 0 | 7.77 | 46.89 | 45.34 | 2.172 | 0.95 |
| 5 | 0 | 0 | 0.03 | 7.61 | 54.43 | 37.93 | 2.223 | 0.94 |
| 6 | 0 | 0 | 0.13 | 6.65 | 41.28 | 51.94 | 2.218 | 0.94 |
| 7 | 0 | 0 | 0.06 | 7.81 | 45.77 | 46.36 | 2.229 | 0.94 |
| 8 | 0 | 0 | 0.10 | 8.78 | 26.69 | 64.43 | 2.368 | 0.91 |
| 9 | 0 | 0 | 0.02 | 4.00 | 55.94 | 40.04 | 2.201 | 0.95 |
| 10 | 0 | 0 | 0.09 | 13.13 | 35.56 | 51.22 | 2.195 | 0.93 |
| 11 | 0 | 0 | 0.03 | 3.12 | 22.00 | 74.85 | 2.331 | 0.90 |
| 12 | 0 | 0 | 0.01 | 10.24 | 42.84 | 46.91 | 2.257 | 0.94 |
| 13 | 0 | 0.01 | 0.03 | 10.12 | 49.60 | 40.24 | 2.282 | 0.92 |
| 14 | 0 | 0 | 0.05 | 15.56 | 45.07 | 39.32 | 2.215 | 0.95 |
| 15 | 0 | 0 | 0 | 4.18 | 55.96 | 39.86 | 2.173 | 0.97 |
| 16 | 0 | 0 | 0.06 | 13.40 | 38.32 | 48.22 | 2.206 | 0.95 |
| 17 | 0 | 0 | 0 | 3.51 | 57.31 | 39.18 | 2.144 | 0.96 |

Note: Layers were numbered from the top (surface soil) to the bottom (subsoil) of the dam land.

Table 4. Annual soil particle size distribution and fractal dimension $D_m$ of the layered sediments from the Shipanmao dam land.

| Deposition year | Sediment layer | Soil particle size distribution (mm) | | | | | | $D_m$ | Determination coefficient $R^2$ |
|---|---|---|---|---|---|---|---|---|---|
| | | Gravel | Coarse sand | | Fine sand | | Silt–clay | | |
| | | 2.0–1.0 | 1.0–0.5 | 0.5–0.25 | 0.25–0.1 | 0.1–0.05 | <0.05 | | |
| 1979 | 1–2 | 0 | 0 | 0.06 | 5.31 | 24.64 | 70.00 | 2.139 | 0.89 |
| 1978 | 3–7 | 0 | 0 | 0.10 | 5.93 | 25.45 | 68.52 | 2.161 | 0.88 |
| 1977 | 8–12 | 0 | 0 | 0.05 | 10.72 | 31.18 | 58.05 | 2.141 | 0.89 |
| 1976 | 13–15 | 0 | 0 | 0.13 | 9.86 | 20.01 | 70.01 | 2.160 | 0.87 |

| | | | | | | | | | |
|---|---|---|---|---|---|---|---|---|---|
| 1975 | 16 | 0 | 0 | 0.06 | 10.00 | 19.69 | 70.25 | 2.171 | 0.86 |
| 1974 | 17–18 | 0 | 0 | 0.06 | 5.27 | 24.48 | 70.20 | 2.161 | 0.89 |
| 1973 | 19–20 | 0 | 0 | 0.07 | 16.37 | 22.94 | 60.63 | 2.147 | 0.87 |
| 1972 | 21 | 0 | 0 | 0.03 | 2.34 | 20.22 | 77.41 | 2.219 | 0.87 |

Table 5. Land use types in the dam-controlled area of the Shipanmao check dam in 1972 and 1979.

| Year | Area ($m^2$) | | | | | |
|---|---|---|---|---|---|---|
| | Sloped farmland | Forest | Grassland | Terrace | Dam land | Badland |
| 1972 | 453,900 | 618,600 | 288,500 | 162,700 | 0 | 480,800 |
| 1979 | 792,500 | 573,000 | 32,800 | 182,700 | 14,400 | 409,100 |
| Increment ($m^2$) | 338,600 | –45,600 | –255,700 | 20,000 | 14,400 | –71,700 |
| Increment (%) | 74.60 | –7.37 | –88.63 | 12.29 | / | –14.91 |
| *C* factor in USLE | 0.310 | 0.006 | 0.154 | 0.310 | 0 | 0.411 |

**Highlights:**

- The soil PSD of layered sediment from dam lands has fractal characteristics.
- The $D_m$ has significant positive, negative correlations with silt–clay, fine sand.
- Factor impacting turning point of $D_m$ is the trends of soil PSDs in adjacent layers.
- The $D_m$ is a useful measurement to judge the impact of land use types.
- PSD is a more dominant factor affecting $D_m$ than the time lag of sediment transfer.